Real-Time Single Trial Phase Synchrony Detection in Physiological Signals

BY

Hafsah Ahmad

(NUST2013362106MSMME62313F)

Supervised by: **Dr. Muhammad Nabeel Anwar**

School of Mechanical and Manufacturing Engineering

National University of Sciences and Technology

H-12 Islamabad, Pakistan

January, 2016

REAL-TIME SINGLE TRIAL PHASE SYNCHRONY DETECTION IN PHYSIOLOGICAL SIGNALS

A thesis submitted in partial fulfillment of the requirement for the degree of

Masters of Science

In

Biomedical Engineering

By

HAFSAH AHMAD
NUST2013362106MSMME62313F

Supervised by: **Dr. Muhammad Nabeel Anwar**

School of Mechanical and Manufacturing Engineering
National University of Sciences and Technology
H-12 Islamabad, Pakistan
January, 2016.

Form TH – 4: Master's Thesis Work

We hereby recommend that the dissertation prepared under our supervision by **Hafsah Ahmad (NUST2013362106MSMME62313F)** titled: **Real-time Single Trial Phase Synchrony Detection in Physiological Signals** be accepted in partial fulfillment of the requirements for the award of MS degree with ___ Grade.

Examination Committee Members

Dr. Syed Omer Gillani _____

Dr. Umer Ansari _____

Dr. Adeeb Shehzad _____

Supervisor

Dr. Muhammad Nabeel Anwar _____

_____

Dr. Muhammad Nabeel Anwar

Head of Department

Biomedical Engineering and Sciences

Date: _____

_____

Principal/Dean

School of Mechanical and Manufacturing Engineering

National University of Sciences and Technology

Islamabad, Pakistan

Date: _____

To

Mama, Abu G, Haris and Hassan

ACKNOWLEDGEMENTS

In numerable thanks to "The ALLAH Almighty" The Merciful and the source of all knowledge and wisdom, who bestowed upon me help, thoughts, talented teachers, opportunities and power of communication.

I owe respectful gratitude and deep sense of obligation to my supervisor Dr. Nabeel Anwar for believing me and giving me a chance to work with him, for his consistent behavior, encouragement, constructive criticism, inspiring guidance, ever friendly attitude and intense co-operation at every stage. Without his guidance this work would not have been completed.

I am grateful from the depth of my heart to Sir Tahir Khalid Butt for his continuous and worthy support, patience, immense knowledge, inspiration, dedication and for being there for me during all stages of my thesis work. I cannot thank enough for his efforts; without his mentorship I wouldn't have learnt as much as I had

I want to thank Dr. Abdul Ghafoor (Principal, School of Mechanical and Manufacturing Engineering, NUST) who's guidance and financial Support encouraged me to work with full devotion and enthusiasm on this project. Special thanks to Engr. Muhammad Asghar, Rector National University of Science and Technology (NUST), for providing a platform full of research opportunities in NUST.

I want to express special thanks to thesis committee members Dr. Syed Omer Gillani, Dr. Adeeb Shehzad and Dr. Umar Ansari for their support, guidance and invaluable suggestions.

Acknowledgments

I would like to acknowledge Samran Naveed, my mentor and lab fellow, for his worthy advices, technical assistance and helpful guidance.

Special thanks to my friends and colleagues Nayab Nawaz, Aqsa Shakeel, Muhammad Waqar Khan and Usman Abid Khan for their sincere support, guidance, care and for providing a friendly and pleasant environment at lab. Special thanks to Nayab Nawaz for keeping our taste buds happy.

I would like to express thanks to my friend Nadia Riaz Bajwa for always being there for me and provide a sincere company through thick and thin during my stay at NUST. I am also thankful to my friend and colleague Bakhtawar Ghafoor for her kind help and cooperation.

I would like to appreciate and thank Faisal Amin for his unconditional support and sincere guidance during my research work.

Last but not least, I want to thank all my class fellows for their cheerful company and consistent help during all these years.

Hafsah Ahmad

Table of Contents

List of Figures

List of Tables

LIST OF ACRONYMS

CC	Cross Coherence
CNS	Central Nervous System
ECG	Electrocardiography
ECoG	Electrocorticography
EEG	Electroencephalography
EMG	Electromyography
EOG	Electro-oculography
FDI	First Dorsal Interosseous
FFT	Fast Fourier Transform
FIR	Finite Impulse Response
HT	Hilbert Transform
IIR	Infinite Impulse Response
MEG	Magnetoencephalography
MI	Mutual Information
Msec	milli seconds
PCC	Phase Cross Coherence
PLI	Phase Lag Index

PLV	Phase Locking Value
qEEG	Quantitative Electroencephalography
SPLV	Single Trial Phase Locking Value
WT	Wavelet Transform

Abstract

Physiological signals are recorded through electrodes that sense electrical activity in the biological systems. Synchronization among physiological signals is important for studying the communication mechanisms occurring within and between different physiological systems (e.g. EEG-EEG or EEG-EMG). The aim of this study is to compute the level of synchronization in physiological signals during single trials in real time.

Synchronization is the rhythmic adjustments of self-sustained oscillators because of coupling (e.g. classic clock pendulum). Phase synchronization is the relative temporal constancy of phases of two physiological signals that shows the electrical/oscillatory activity in the body. This oscillatory/electrical activity is called "phase locked" if it occurs time-locked to a stimulus event. A method called Single Trial Phase Locking Value (SPLV) is used in this study for computation of synchrony levels among physiological signals during single trials in real-time.

Two types of physiological signals i.e. EEG and EMG are used in this study. First, SPLV method was developed for offline studies of phase synchronization for EEG data. Based on SPLV results for offline data, SPLV offline method was optimized for use in real-time. For real-time, EEG and EMG signals were used following a finger tapping protocol. For EMG, SPLV's were computed by placing electrodes at mid-belly point and First Dorsal Interosseous (FDI) muscles of both hands. For EEG, electrodes were placed at left and right sensory motor cortex (C3 and C4 according to international 10-20 system). Subjects were asked to perform the same finger tapping task.

Abstract

Real-time single trial phase synchronization can be used to study the plasticity induced in different parts of the brain. This study can be further utilized for neuro-muscular studies for rehabilitation applications. This method can also be used to study diverse functions such as motor activity, working memory, associative memory, attention, object recognition, awareness, perceptual organization or muscular activity during a specific task in real-time.

PART I

INTRODUCTION & LITERATURE REVIEW

1. Electrophysiology

Biological cells and tissues exhibit electrical properties. The study of these electrical properties is known as Electrophysiology. It comprises measuring the changes in voltage or electric current on various scales ranging from single ion channel proteins to entire organs like the heart or brain. The term Electrophysiology is defined Scanziani et al as:

"Electrophysiology is the science and branch of physiology that pertains to the flow of ions (ion current) in biological tissues and, in particular, to the electrical recording techniques that enable the measurement of this flow." (Scanziani & Hausser, 2009)

Two types of electrophysiological signals are focused in this study; Electroencephalography and Electromyography. In neuroscience, it involves measurement of action potential activity of neurons produce electrical signals. When electrical activity of a large network of neurons is measured, it is called Electroencephalography. Similarly, recording the electrical activity produced by action potentials in muscles is called Electromyography. The classical method for measurement of electrophysiological signals is placing electrodes on variety of preparations for biological signals.

1.1 Physiological Signals

Electrophysiological recordings are generally termed as Electrography ("electro" meaning "electrical" and "graphy" meaning "recording"). The recorded signal obtained is called Electrogram. The term Electrography is a general term and may also refer to other types of recording such as Electrophotography. Therefore, to specify electrophysiological signals, they are usually called by specified name in a pattern i.e. electro- + [specify body part] + -graphy (abbreviated as ExG). Generally, electrogram refers to electrocardiogram

that has been recorded by invasive placing of electrodes (Kim, Bang, & Kim, 2004). Table 1 shows different modes of "ExG" signals.

Table 1: Types of Physiological Signals

Modality	Abbreviation	Body Part	Grade
Electrocardiography	ECG or EKG	Heart (cardiac muscle), with cutaneous noninvasive electrodes	3
Electroencephalography	EEG	Brain (cerebral cortex), with extracranial electrodes	3
Electromyography	EMG	Muscles from the whole body (skeletal and smooth muscles)	3
Intracardiac electrogram	EGM	Heart (specifically, the cardiac muscle), with intracardiac electrodes (invasive)	2
Electrocorticography	ECoG	Brain (cerebral cortex), with intracranial electrodes	2
Electrooculography	EOG	Eye (full globe)	2
Electroretinography	ERG	Eye (retina)	2
Electronystagmography	ENG	Eye (via the corneoretinal potential)	2

Electrocochleography	ECOG or ECochG	Cochlea	2
Electrogastrography	EGG	Stomach (smooth muscle)	2
Electrogastroenterography	EGEG	Stomach and bowel (smooth muscle)	2
Electroatriography	EAG	Cardiac muscle (atrial)	1
Electroventriculography	EVG	Cardiac muscle (ventricular)	1
Electroglottography	EGG	Glottis	1
Electropalatography	EPG	Tongue (palatal contact)	1
Electroblepharography	EBG	Eyelid muscle	1

Physiological signals can be recorded at three different levels from the body depending upon the placement of electrodes. These three levels are as under;

a. Cellular
b. Invasive
c. Non invasive

1.2 Electroencephalography (EEG)

1.2.1 Introduction

Electroencephalography (EEG) is a monitoring method for electrophysiological signals to record electrical activity of the brain. It is generally noninvasive, which means electrodes

are placed along the scalp. However, invasive method for placing electrodes is sometimes used in specific conditions. EEG records voltage variations produced from ionic current within the neurons of the specific part of brain (Niedermeyer & da Silva, 2005). For clinical applications, EEG denotes the recording of the brain's impulsive electrical activity for a specified period of time, which is recorded from numerous electrodes placed on the scalp. The applications in diagnostic domain are generally focused on the spectral study of EEG, i.e. the spectrum type of neural oscillations (known as "brain waves") that is a prominent feature in EEG signals.

1.2.2 Origin of Brain Waves

When thousands or millions of neurons fire together, they generate electrical potentials. These electrical potentials can be recorded inside brain, surface of the brain and even on the scalp. These electrical signals recorded corresponds to the oscillatory activity of the brain and therefore these are called “brain waves”. When these brain waves are recorded from scalp using noninvasive surface electrodes, they are called EEG (Electroencephalographs) and their study is called Electroencephalography. Brain waves cannot be recorded for a single neuron on the scalp. This activity is always recorded for a whole network of neurons oscillating at a specific time. More the number of neurons, better will be the electrical activity recorded at scalp.

1.2.3 Signal Characteristics

EEG recordings are usually defined by two major phenomena; rhythmic activity and transients. When the recorded signals are classified according to the frequency bands, it is called the rhythmic activity. The frequency bands are given specific names like alpha, beta,

theta and delta bands. Each frequency band is found to have specific distributions over the scalp and are also biologically significant. Spectral methods are used to extract these frequency bands from raw signals. Certain signal processing tools are available for this purpose like EEGLAB for MATLAB or Neurophysiological Biomarker Toolbox. Computational signal analysis and processing of EEG signals is often termed as Quantitative Electroencephalography (qEEG).

Broad frequency range for most of the cortical signals is reported between 1-40 Hz frequency bands. Frequencies above or below this range are often discarded because they likely occur as a result of certain artifacts when standard clinical methods are used to record signals. This frequency spectrum is then subdivided into narrow frequency bands depending on the origin and brain activity for which signals are recorded. These signals are weak signals in terms of voltage. Their voltages range from 0-200 uV (Tatum, 2014). Table 2 shows the detailed specifications of these narrow frequency bands along with their voltage levels, origin and brain activity during which they might occur.

Table 2: Frequency bands for brain waves

Wave	Amplitude	Frequency (Hz)	Origin	Activity
Alpha	30-50 uV p-p	8-13	Occipital (Intense) Parietal Frontal	Eye close Relaxing
Beta	<20uV p-p	15-30	Parietal Frontal	Mental Activity
Theta	<100 uV p-p	4-7	Parietal and Temporal (Young children	Drowsiness, Arousal (Young children) •Emotional stress, frustration,

				disappointment (Adults)
Delta	100-200 uV p-p	<4	Frontal (Adults) Posterior(Children)	Deep Sleep Infancy
Mu	30-50 uV p-p	8-13	Sensorimotor cortex	Motor Activity Motor imagery

1.3 Electromyography (EMG)

1.3.1 Introduction

Electromyography is the technique that records muscle activity. Muscle activity may occur as a response to electrical activity inside muscle fibers, stimulation of muscle due to a nerve impulse at rest and during muscle movements involving contraction and relaxation. EMG signals are acquired using surface electrodes that can be placed on a certain body muscle (noninvasive). Muscle should exhibit no electrical activity when electrodes are placed on a muscle at rest. Since a noise factor is always present while recording signals, a white noise can be seen as an output for a muscle at rest (Siriprayoonsak, 2005). Whenever, there is an activity in muscle, it contracts due to action potentials generated within muscles that will produce electrical activity. The strength of this electrical activity depends on the extent to which muscles contract (Bronzino, 1999).

EMG signals are found clinically useful in the diagnosis of neuromuscular diseases, neuropathic diseases and myopathic diseases. Along with clinical applications, EMG signals are also very useful in the field of prosthetics; to control prosthetic devices like prosthetic limbs (Herrera, Bernal, Isaza, & Adjouadi, 2004). EMG signals have a wide range of applications in the field of robotics as well. They can be used to control computers and other gadgets. Devices are available with EMG based interface and are used to control

mobile robots and electric wheelchairs. Muscle-computer interface can be used to move mouse pointers and play interactive video games.

1.3.2 Origin of Electromyograms

Electrical excitation of skeletal muscle is initiated and regulated by the central and peripheral nervous systems. The signals are originated at the junction of Nerves and muscles called motor points. Whenever the brain sends a contraction signal through nerves to the muscles, an electrical activity is generated in the muscles because of action potentials generated in muscles and thus EMG is originated. That's why these signals are called Neuro-Muscular signals. An electrode placed on the motor point of that muscle will record this electrical activity. The strength of electrical activity depends on the extent to which muscles contract and the strength of muscle as well. Figure 1 shows the mechanism through which EMG signals are originated and recorded.

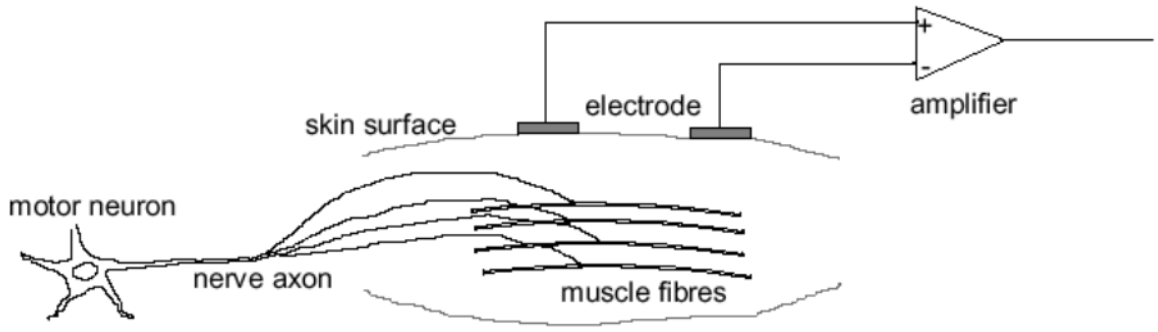

Figure 1 Origin of muscle signals

1.3.3 Signal Characteristics

A raw EMG signals is a bipolar signals having random fluctuations that has been acquired using surface electrode placed on muscle (Lamb & Hobart, 1992). The voltage

levels typically range form 2-10 mV before amplification. The frequency band that contains the usable information is a wide frequency band ranging from 0-500 Hz. This means the significant energy of the signal is above the level of electrical noise in the frequency band. Generally, the dominant energy of EMG signals lies between 50-150 Hz frequency band (Nawab, Wotiz, Hochstein, & De Luca, 2002). Figure 2 shows the raw EMG signal in time domain and its corresponding frequency domain signal. It can be seen that the dominant energy is in the lower frequencies.

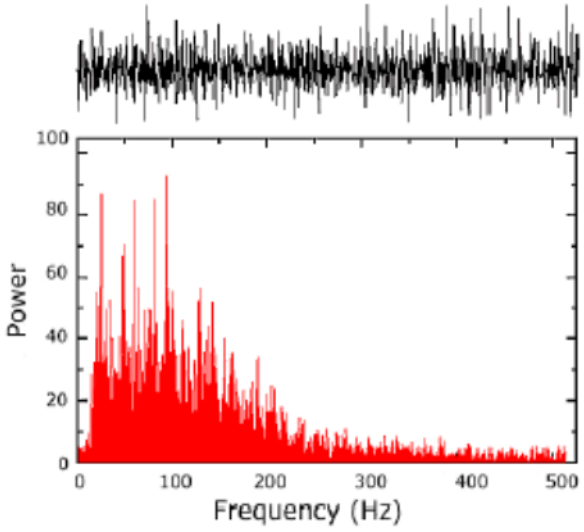

Figure 2: Raw EMG signal (black) and corresponding frequency spectrum (red)

2. Synchronization

Synchronization is a phenomenon in physics having a long tradition, starting from the observation of two oscillating pendulums at a time by Huygens in 1665. Synchronization is a nonlinear phenomenon observable in several natural and technical systems, including the biological aspect of human brain (Jovanov et al., 2003).

Synchronization can be explained as the rhythmic adjustments of self-sustained oscillators as a result of coupling. A self-sustained oscillator can be defined as a dynamic system capable of generating oscillations out of itself instead of being stimulated by an external rhythm. A very basic example of oscillatory self-sustained system is classic clock pendulum. It is self-sustained in the sense that it has an internal energy reservoir comprising of weights. The periodic oscillatory motion of pendulum is generated by utilizing this energy. Amplitude and frequency of oscillations are the two basic phenomenon of the pendulum clock mechanism. Amplitude and frequency of oscillating body will remain constant under ideal conditions (no friction).

Synchronized oscillatory activity can also be understood by taking example of two simple pendulums. A simple pendulum is a mass "m" attached to a fixed point via cable of length "l" and oscillating along x-axis making an angle "θ" with the ground. When two simple pendulums; 1 and 2; oscillate together making an angle "θ_1 "and "θ_2 "respectively at any instant of time "t", they are said to be synchronous. This situation is explained in the Figure 3 below;

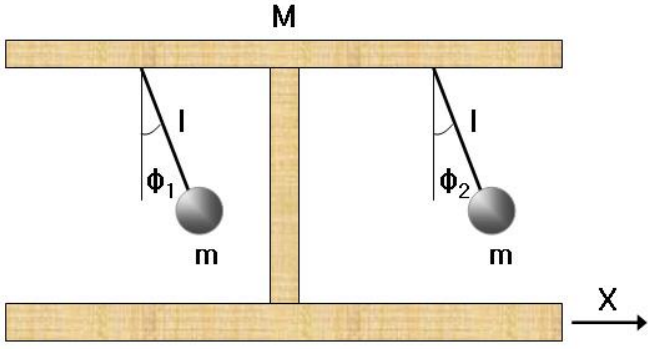

Figure 3: Synchronization pattern for simple pendulum

2.1 Phase Synchronization

The phenomenon of synchronization can be seen in nature in all living organisms. This phenomenon is used on a large scale by researchers to study different natural phenomenon occurring in different organs of the body. The part of body for which synchronization phenomena is observed is actually a natural "sub-system". This helps researchers in studding interaction between natural sub-systems. Synchronization between signals can be studied for two features; amplitude and phase". Amplitude synchronization corresponds to synchronization between networks (neurons or muscle fibers). Phase synchronization corresponds to frequency of firing rates (action potentials). This study focus only on phase synchronization between physiological signals (EEG and EMG).

Phase synchronization in terms of physiological signals can be defined as;

"Phase synchronization is locking of the phases of two physiological signals that shows the electrical/oscillatory activity in the body." (Varela, Lachaux, Rodriguez, & Martinerie, 2001).

Let there be two electrodes I and j, placed at two different regions of a natural sub-system (brain or muscles), the difference of phase between these two signals can be showed as:

$$\varphi_{i,j} = n\varphi_i(t) - m\varphi_j(t) = constant$$

where n and m are integers, φ_i and φ_j denote the phases of the electrodes I and j, and $\varphi_{i,j}$ is defined as their relative phase. High values of $\varphi_{i,j}$ (that is, close to 1) indicate that "i" reproduces the variations of j, with a time lag t that can be different from zero (König, Engel, Roelfsema, & Singer, 1995). Similarly, if one is interested in the relation between the signals at a specific frequency f, one can band-pass signals from i and j

narrowly around f, and estimate their coherence, which is simply the correlation coefficient between the band-passed signals.

In order to investigate synchronization of chaotic systems, Rosenblum et al. (Rosenblum, Pikovsky, & Kurths, 1996) replaced this condition of phase locking by the weaker condition of phase entrainment:

$$\left|\varphi_{i,j}\right| = \left| n\varphi_i(t) - m\varphi_j(t)\right| < constant$$

Synchrony measures the relation between the temporal structures of the signals regardless of signal amplitude. Two signals are said to be synchronous if their rhythms coincide. This idea can be made more precise in several ways. In its classical sense, the term synchrony has been applied to signals that had a dominant oscillatory mode, either originally or after filtration around a chosen frequencyω. Such signals can be written in frequency domain with the even weaker condition of frequency locking (Mormann, Lehnertz, David, & Elger, 2000)

$$\langle\omega_{i,j}\rangle = n\langle\omega_i\rangle - m\langle\omega_j\rangle$$

$$= n\left\langle\frac{d\varphi_i(t)}{dt}\right\rangle - m\left\langle\frac{d\varphi_j(t)}{dt}\right\rangle - 0$$

where $\langle\ \rangle$ denotes averaging over time, and $\omega_{i,j}$ the relative frequency of the systems.

2.2 Phase Synchronization in Physiological Signals

The concept of phase synchronization is used on a large scale to study the interaction between different physiological signals. In case of EEG, phase synchronization is used to study interaction between different cortical areas; both on inter-hemispheric and intra-hemispheric levels. This shows how different cortical regions interact in order to complete

a specific task like learning or a motor task. In case of EMG, phase synchronization concept is used to study how different muscle pairs interact during a specific task. The level of phase synchronization thus obtained indicates how muscle pairs are activated.

2.2.1 Phase Synchronization in EEG

Phase synchronization in EEG has been used by researchers to study interaction between different cortical regions. Almost all of these studies are conducted offline; i.e. signal analysis is performed on recorded signals. Learning and cognition is a hot research area and researchers have used phase synchronization to study increase or decrease in learning during different mental tasks (Chen, Madhavan, Rapoport, & Anderson, 2013; Glennon, Keane, Elliott, & Sauseng, 2015; Lachaux et al., 2000; Sadeghi, MacKay, van Dam, & Thompson, 2011). Motor activity and motor imagery has also been studied to study interaction between different parts of sensorimotor cortex during various tasks (Hsu, 2013; Krusienski, McFarland, & Wolpaw, 2012). These signals are not only important for research purpose, but are also used clinically for the detection of mental diseases like Parkinson's (Ahn, Zauber, Worth, Witt, & Rubchinsky, 2015; Swann et al., 2015), Strokes (Ewen et al., 2015; Lei Wang, Guo, Sun, Jin, & Tong, 2012), Alzheimer (Knyazeva et al., 2013), Epilepsy (Vecchio et al., 2015),

2.2.2 Phase Synchronization in EMG

Phase synchronization concept is also widely used for EMG signal analysis. A key feature of dominant mechanisms for processing of information from motor activities is impulsive oscillatory activity. This activity can be distinguished using physiological signals i.e. electroencephalographic (EEG) and electromyographic (EMG) signals

(Boonstra & Breakspear, 2012). Paired EEG–EMG and EMG–EMG synchronization study have been applied to evaluate the muscular oscillatory input to the motor units (Lejun Wang et al., 2015). Specifically, synchronization pattern of synergistic and homonymous motor unit activation is caused by common synaptic input from the last order neuronal branches to the motor neurons of spinal cord (Keen, Chou, Nordstrom, & Fuglevand, 2012). This can be computed using EMG–EMG coherence or phase synchronization analysis methodologies. EMG–EMG coherence computes the common oscillatory drive to muscular co-contraction or to two fragments of the particular muscle (Farmer, 1998; van Asseldonk, Campfens, Verwer, van Putten, & Stegeman, 2014). Earlier researchers have showed that intermuscular and intramuscular coherence in frequency bands of beta (15–35 Hz) and gamma (35–60 Hz) are mainly caused by motor cortex (Chang et al., 2012). However, coherence in alpha band (8–12 Hz) is caused due to certain other reasons (McAuley & Marsden, 2000). Not only coherence method in frequency domain has been used, there are several studies that detected a phase lag among the EEG and EMG recordings (Halliday, Conway, Farmer, & Rosenberg, 1998). Also, both signals are phase locked (phase synchronized) (Ushiyama et al., 2011). This shows that phase synchronization of EMG signals among muscular co-contractions might show information about cortical-related modulation. Common oscillatory drive is found to be very closely related to the actions of cortico-motoneuronal cells found in cortex. Their activity is synched with action potentials of motor units in groups of instantaneously active muscles (McKiernan, Marcario, Karrer, & Cheney, 2000). This proposes that there exists a close relation among EMG–EMG synchrony and central descending drive among pairs of agonist and antagonist muscles.

3. Methods for the Evaluation of Phase Synchronization

Numerous different methodologies have been used for the computation of synchronization among oscillating signals. Among these methods, most successful are the Phase Locking value (PLV) method,(Aydore, Pantazis, & Leahy, 2013; Lachaux, Rodriguez, Martinerie, & Varela, 1999; Tass et al., 1998) and Phase Cross Coherence (PCC) method (Mormann et al., 2000; Varela et al., 2001). In PLV approach, the phases of oscillating signals are computed using wavelet transform (WT) analysis or by using the analytical signal computed through the Hilbert transform (HT) (Pfurtscheller & Da Silva, 1999). These methods are developed to obtain the phases between pairs of oscillating signals inside a moderately narrow frequency bandwidth, and to compute synchronization among those oscillating signals by computing the extent of constancy of the phase relationship among the two signals. Alternative methods are present for the quantification of synchronization between oscillating signals, such as Mutual Information (MI), Shannon Entropy (SE), and synchronization likelihood methods (Hurtado, Rubchinsky, & Sigvardt, 2004; Mormann et al., 2000; Yeung, Bogacz, Holroyd, & Cohen, 2004).

PART 2

METHODOLOGY

Single-trial Phase Locking Value (SPLV) approach was selected for the computation of phase synchronization in this study. Prior to implementation of system in real-time, offline algorithm was developed. This is a common practice to develop offline algorithm before switching to real-time implementation as evident from previous studies (Brunner, Scherer, Graimann, Supp, & Pfurtscheller, 2006; Quiroga, Kraskov, Kreuz, & Grassberger, 2002; Sadeghi et al., 2011). For offline system development, SPLV algorithm was first implemented on simulated signals and then on recorded physiological signals (EEG and EMG) during different tasks. The same system was then implemented in real-time to compute the level of synchronization for physiological signals. This section discusses in detail the methodology used for both offline and real-time system implementations.

This section is divided into two parts, offline phase and real-time/online phase as shown in the block diagram below;

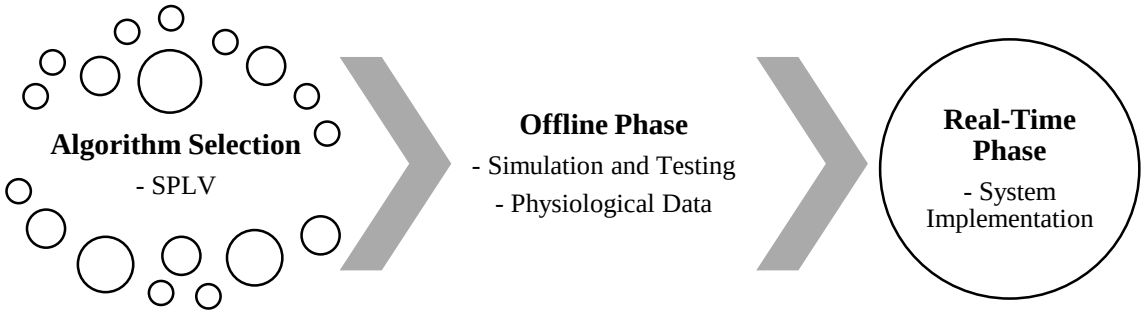

Figure 4: System Flow Chart

4. Algorithm Selection

Among several techniques used for the quantification of phase synchronization, PLV and PCC were found to be efficient methods as mentioned in previous studies (Aydore et al., 2013; Chang et al., 2012; Doesburg & Ward, 2009). These two methods, and some other methods available for the calculation of phase synchronization are equally applicable for offline phase synchronization computation. For real-time implementation of a system, generally there are factors like computational cost and temporal delay that have to be considered. A method with least computational cost and hardware with minimum temporal delays is the main goal of study. Keeping these scenarios in mind, Phase Locking Value method was found to be the best for implementation in a real-time system. Phase Locking Value takes into account only the instantaneous phase of the signal, therefore reducing the computational cost. Evidences are present in literature for the reliability of this method during online phase synchronization analysis (Aydore et al., 2013; Brunner et al., 2006; Chen et al., 2013; Sadeghi et al., 2011; Y. Wang, Hong, Gao, & Gao, 2006).

4.1 Single-trial Phase Locking Value

Phase Synchronization Value (PLV) has been widely used for the computation of phase synchrony among physiological signals. This method is regarded as the best method for task dependent physiological signals (EEG and EMG). PLV quantifies the spontaneous relation between the phases of two signals at a given time. This instantaneous phase relationship is then averaged either over the total number of trials or over the total number of time points. When averaging is done over total number of trials that are time locked to a repetitive event, it is called Phase Locking Value (PLV). PLV is a multi-trial

computational method in this study, averaging is done over total number of time points and is thus called Single-trial Phase Locking Value (SPLV).

Suppose two real signals $s_1(t)$ and $s_2(t)$ that are physiological signals acquired using the surface electrodes 1 and 2, places on two different points of the body part under observation. Suppose also that these signals are pre-processed and filtered in the frequency band of interest (alpha, beta, gamma or delta). Analytical signals for $s_1(t)$ and $s_2(t)$ will be;

$$z_i(t) = A_i(t)e^{j\varphi_i(t)}$$

For $i = \{1\ 2\}$ for signals from electrode 1 and 2, and $j = \sqrt{-1}$. $A_i(t)$ Is the analytical signal obtained using the Hilbert Transform (HT) as?

$$A_i(t) = s_i(t) + jHT(s_i(t))$$

where $jHT(s_i(t))$ is the Hilbert transform of $s_i(t)$ defined as;

$$HTs_i(t) = \frac{1}{\pi} P.V. \int_{-\infty}^{\infty} \frac{s_i(t)}{t-\tau} d\tau$$

and P.V. represents Cauchy principal value. After obtaining analytic signals, the relative phase between signals can be calculated as

$$\Delta\varphi(t) = arg\left(\frac{z_1(t)z_2^*(t)}{|z_1(t)||z_2(t)|}\right)$$

Using this relative phase, instantaneous PLV is computed as suggested by Lachaux et al. (Lachaux et al., 1999) as

$$PLV(t) = \left|E\left[e^{j\Delta\varphi(t)}\right]\right|$$

Here E[.] represents the Expectation value. PLV values range between [0 1], where 0 corresponds to no synchronization in phase values and 1 corresponds to the signals those are perfectly phase synchronized. In this study, Hilbert Transform is used to compute analytical signal. However, continuous Morlet wavelet transform approach can be used to obtain complex signals producing separate band pass filtered for individual scales of wavelet transform.

Instantaneous PLV's are averaged over total number of trials or time points to obtain a single PLV value (Lachaux et al., 2000; Lachaux et al., 1999; Liang, Choi, Qin, Pang, & Heng, 2014; Yeung et al., 2004). The non-parametric estimation factor can be replaced by a averaging the instantaneous phase differences over the total number of trials as shown below;

$$PLV = \left| \frac{1}{N} \sum_{n=1}^{N} e^{j\Delta\varphi_i(t)} \right|$$

where n indexes the trial number and N is the total number of trials. $\Delta\varphi_i(t)$ Is the instantaneous phase difference i.e. $\Delta\varphi_i(t) = \varphi_1(t) - \varphi_2(t)$.

For the calculation of single trial phase locking value SPLV, averaging is done over time points instead of averaging over epochs or trials. SPLV is calculated by taking a time of few hundreds of milliseconds before and after the trigger (stimulus). Data at the start and end of EEG signal is redundant and is automatically rejected when a filter of higher order is applied. For SPLV, the equation will become,

$$SPLV = \left| \frac{1}{T} \sum_{t=1}^{T} e^{j\Delta\varphi_i(t)} \right|$$

where T is the total time period of a single epoch, and t is the time instant for which SPLV is computed. SPLV computation steps are shown in the block diagram below which is a summary of steps explained mathematically here.

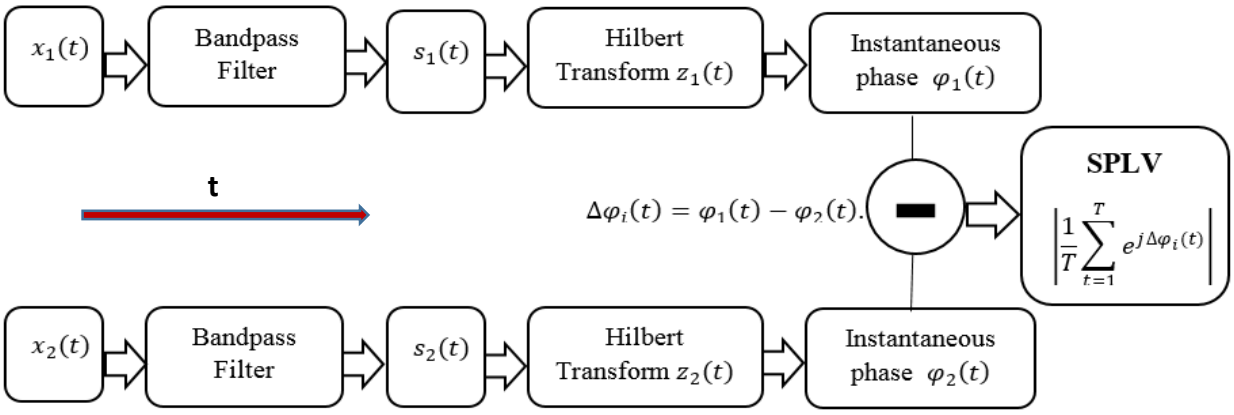

Figure 5: SPLV Block diagram

5. Offline Phase

An efficient working offline system development is always the first step before implementing a system in real-time. For this purpose, the selected algorithm i.e. SPLV was first implemented on a simulated data and results were analyzed. This algorithm was then used to detect the phase synchronization on recorded physiological signals. These signals were EEG signals recorded during visuomotor task for a previous study (Anwar, Navid, Khan, & Kitajo, 2015).

5.1 Simulation

To simulate physiological signals offline, two sinusoidal signals were simulated. Each sine wave corresponding to data acquired from a sensor for physiological signal. Two sine waves $a_1(t)$ and $a_2(t)$ were created with similar amplitude (amp=1) and for a time period of 2 seconds (2000 msec). $a_1(t)$ had a fixed frequency of 10 Hz throughout the time period. $a_2(t)$ was simulated such that it had varying frequencies between 8-13 Hz (alpha rhythms). Each random frequency in this band was assigned for a period of 200 msec. This means there were total 10 frequencies in $a_2(t)$ between 8-13 Hz for a period of 2 seconds.

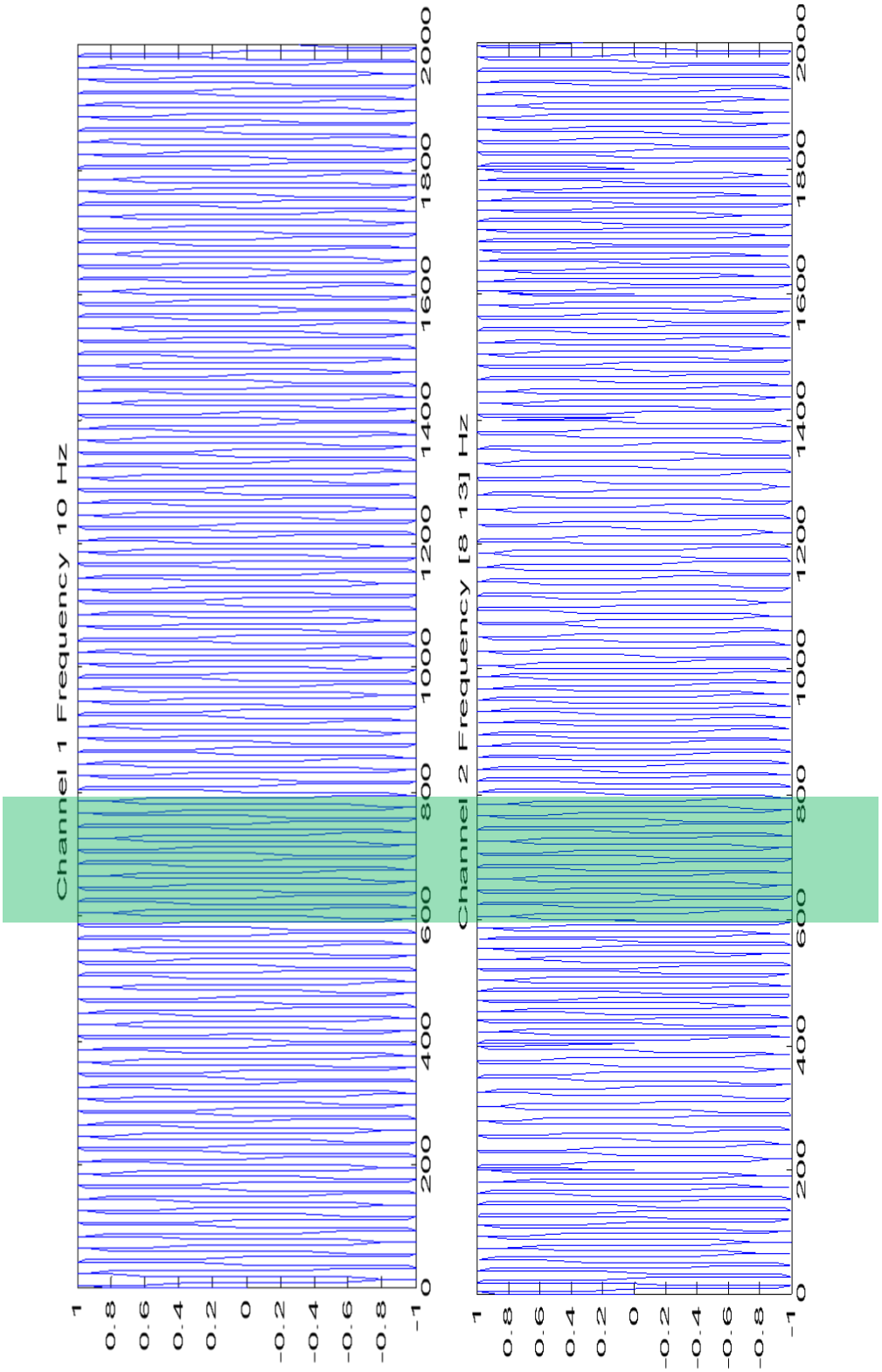

Figure 6: Simulated Signals for Channel 1 and Channel 2. Highlighted portion shows the region where frequency is kept constant (10 Hz)

In the figures above, Channel 1 corresponds to $a_1(t)$ and Channel 2 corresponds to $a_2(t)$. As mentioned earlier, SPLV measures the extent to which phase (frequency) remains locked during a specified time interval. This means that SPLV will be maximum during the time interval when frequencies of both channels is constant. To evaluate this, frequency was set to 10 Hz during 600-800 msec interval for $a_2(t)$ shown in the bounding box in above figure. Frequency domain plots (FFT) for both channels $a_1(t)$ and $a_2(t)$ are shown in Figure 7 below.

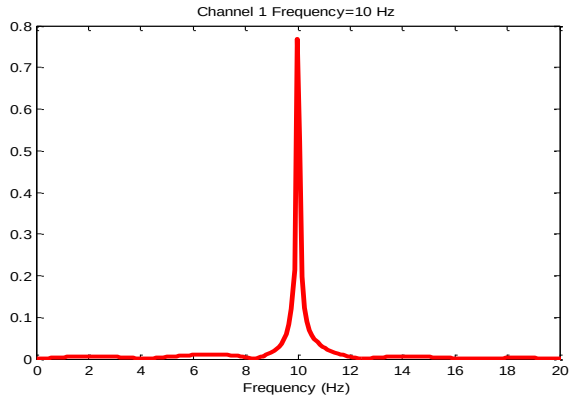

Figure 7 Channel 1 FFT

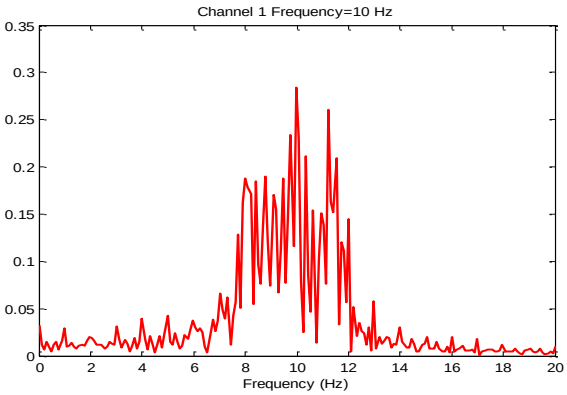

Figure 8 Channel 2 FFT

SPLV's were computed for each 200 msec interval for both channels $(a_1(t), a_2(t))$ and the results were analyzed.

5.2 EEG Data

After the successful results for simulated data, SPLV was applied on offline EEG data. This data was recorded during a visuomotor task for the study of Anwar et al. (Anwar et al., 2015). A summary of experiment for recording this data is mentioned here for instance. The study was composed of two experiments and evaluating nonverbal components of the revised Wechsler Adult Intelligence Scale (WAIS-R). In the first experiment, the ability to suppress movement related motor rhythms was evaluated using EEG. In the second experiment, motor adaptation as the perceptual motor ability of aiming (i.e. the ability to rapidly and accurately move the dominant hand towards a small target) was evaluated by introducing visuomotor perturbations during reaching movements. For each participant the experiment 1 and 2 was conducted on same day while WAIS-R was administrated on a different day. During the experiment, the subject was asked to hit a target appearing on a screen with the help of a stylus pen placed on a tablet. The target appeared on different positions in the screen and the task was to hit the target within given time interval. Figure 9 shows the experimental setup for recording this data.

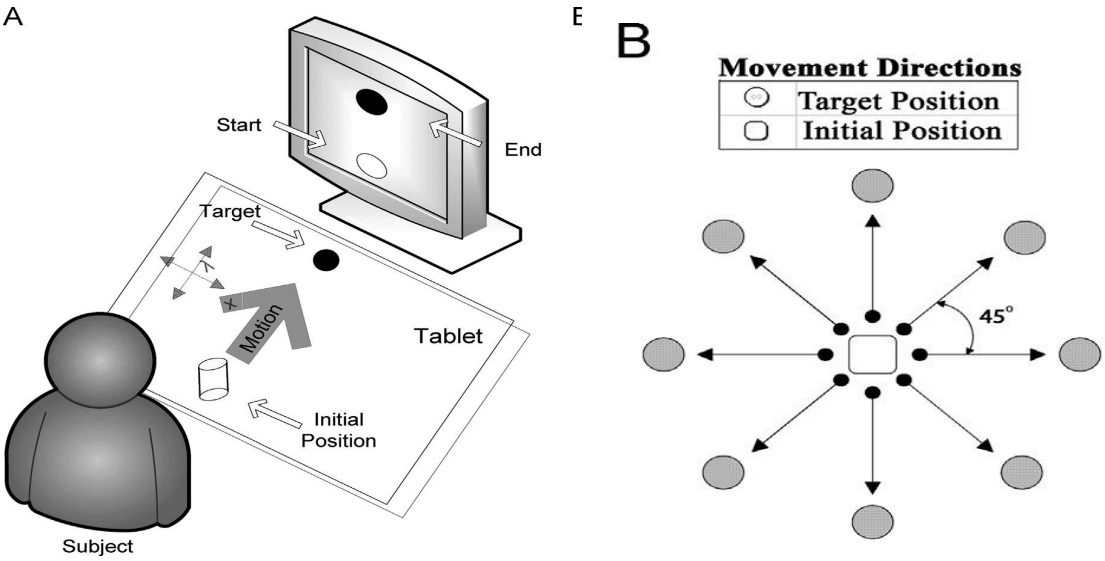

Figure 9: Visuomotor Task for EEG data (Anwar et al., 2015)

5.2.1 Data Specifications

EEG data used for computation of offline SPLV was a three dimensional 64 channel data with 512 trials (epochs). Each trial was 2.5 seconds long. 64 channel data corresponds to 64 cortical positions on brain as decided by International 10-20 system (Herwig, Satrapi, & Schönfeldt-Lecuona, 2003; Okamoto et al., 2004). 64 electrodes were placed at these positions. Cortical area position and corresponding electrode number at each position are shown in the figure below;

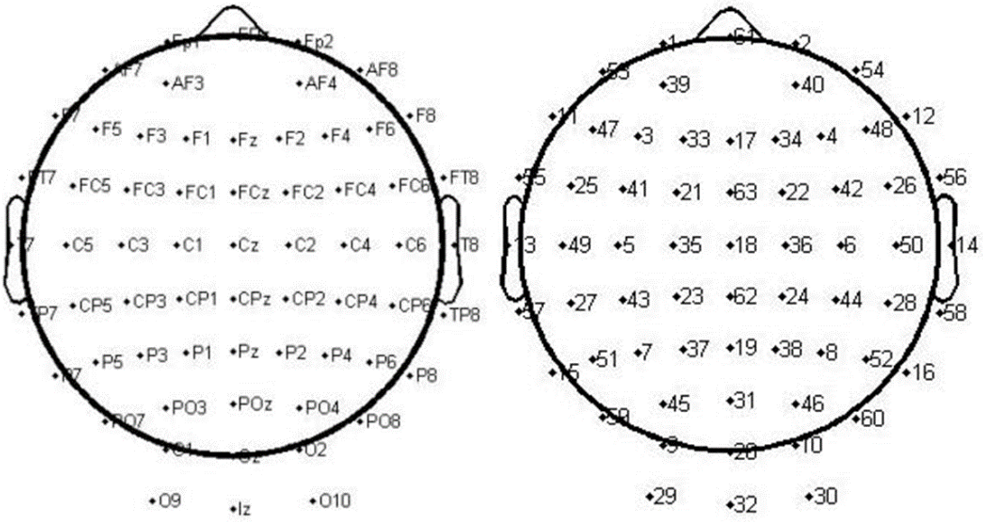

Figure 10: Channel locations according to 10-20 system and corresponding electrode numbers

Sampling rate was set to 500 Hz. Each trial start at 0 sec and ends at 2.498 sec. This means there are total 1250 frames or time points and each time point corresponds to 2 msec of data. Complete specifications of data are shown in table below.

Table 3: EEG Data Specifications

Parameter	**Specification**
Channels	64
Sampling Rate	500
Epochs	512
Time per epoch	2.5 seconds

Frames per epoch	1250
Epoch Start Time	0.000 seconds
Epoch End Time	2.498 seconds

5.2.2 Software

MATLAB® (Matlab Inc.) was used for the computation of SPLAV. Matlab DSP (Digital Signal Processing) toolbox was used for the signal processing part and EEGLAB toolbox was used for initial analysis of offline EEG data.

5.2.3 Single Trial Analysis

For each single trial, stimulus or trigger was given at 750th time point. From literature, it is proved that a time period of few hundred milliseconds before and after the stimulus is used for calculating SPLV (Doesburg & Ward, 2009). In this case, two time windows were created and were named as “pre-trigger window” and “post-trigger window”. Pre-trigger window constituted of time interval 550-749 time points (1 time point = 2 msec) and post-trigger window constituted of time interval 751-950 time points. This means that SPLV was computed 400 msec before and 400 msec after trigger. A single trial, single channel raw data is shown in the figure below. Trigger point and pre-trigger and post-trigger windows are highlighted in this figure.

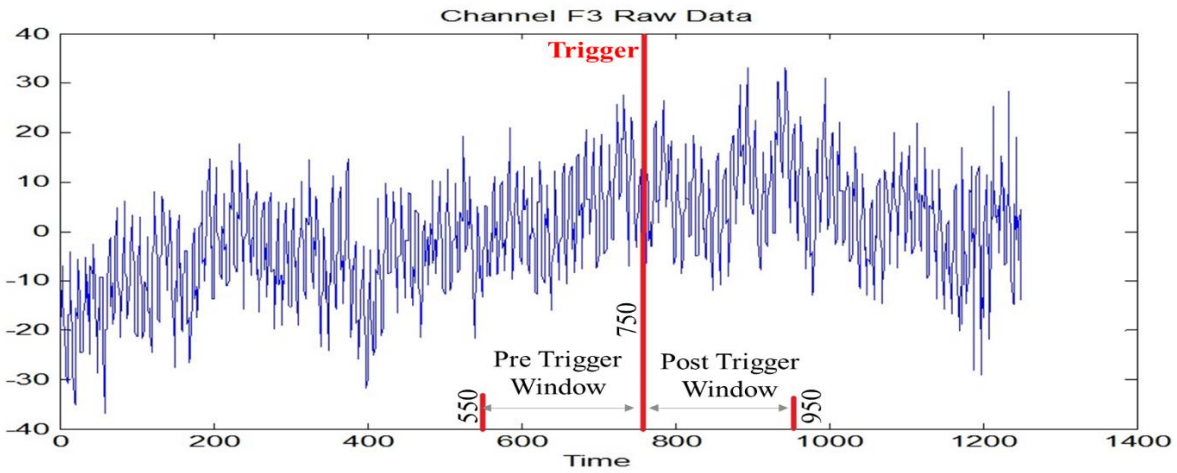

Figure 11: Visualization of single channel, single trial data

Epochs or triggers were divided into three learning phases and were named pre-learning phase, learning phase and post-learning phase according to the protocol. Table below shows the distribution of trials in accordance with three learning phases.

Table 4: Trial Distribution

Phase	Trial Number
Pre- Learning	1-192
Learning	193-420
Post-Learning	421-512

Averaged SPLV's were calculated for each learning phase for seven different channel pairs to check the brain connectivity during the visuomotor task. These channel pairs were selected to study the connectivity between left and right motor cortex, left and right parietal cortex, frontal and parietal cortex, left and right frontal cortex, two pairs of neighboring channels and a pair of channels that are far away spatially. Spatially close channel pairs were selected to examine either there is cross talk between neighboring

electrodes or not. Spatially far away channels were also examined to show the low connectivity between two inactive channels. These channel pairs are as follows;

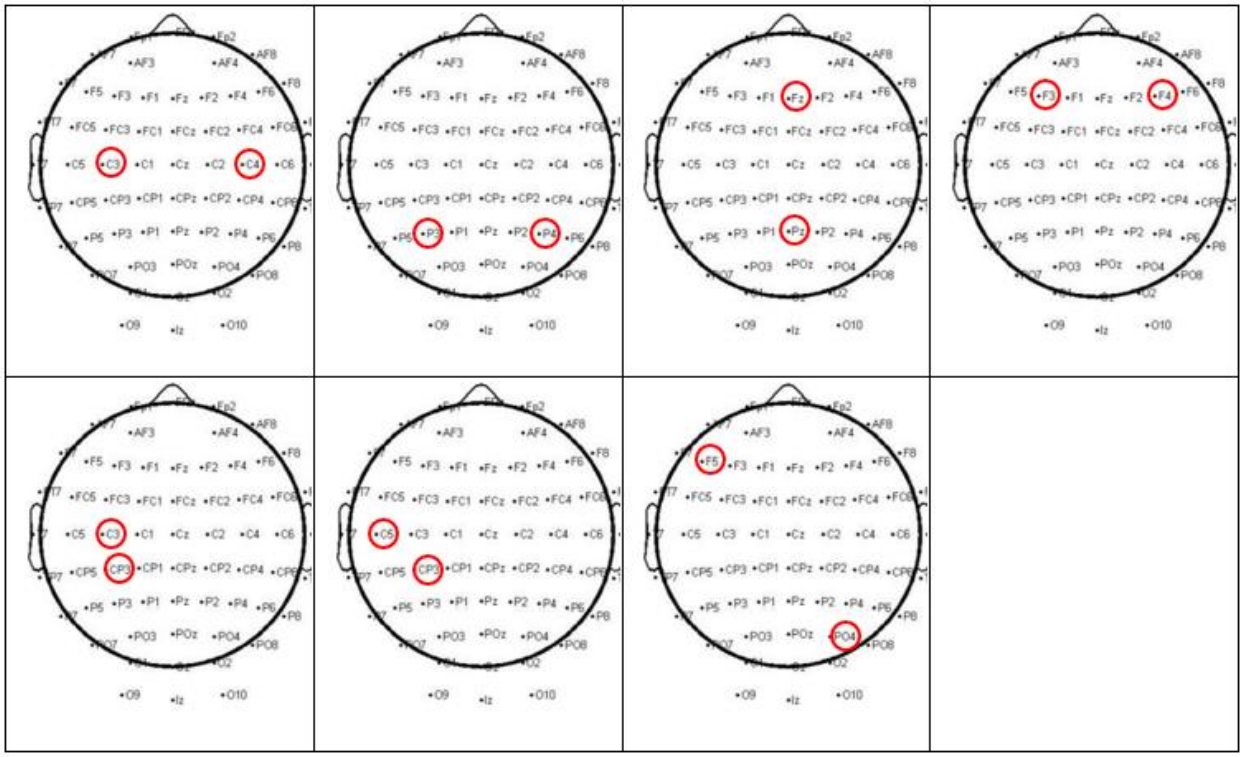

Figure 12: Selected channel pairs for SPLV computation

6. Real-time Phase

After testing SPLV methodology on simulated data and offline EEG data, the same algorithm was implemented in real-time for EEG and EMG signals. The offline algorithm developed was made optimal to work efficiently for real-time system. While working in a system in real-time, major challenges are to handle computational cost, time lags and run-time errors. Therefore, SPLV method was kept simple to have least computational cost. EEG and EMG signals were provided to the system and SPLV's were displayed in real-

time. This section discusses the real time system, hardware and task for EEG and EMG signals in detail.

6.1 System Overview

Figure 13 shows the overall real-time implementation. CH1 and CH2 corresponds to signals acquired from two electrodes placed either on scalp (EEG) or on muscles (EMG). Each block is discussed in detail below.

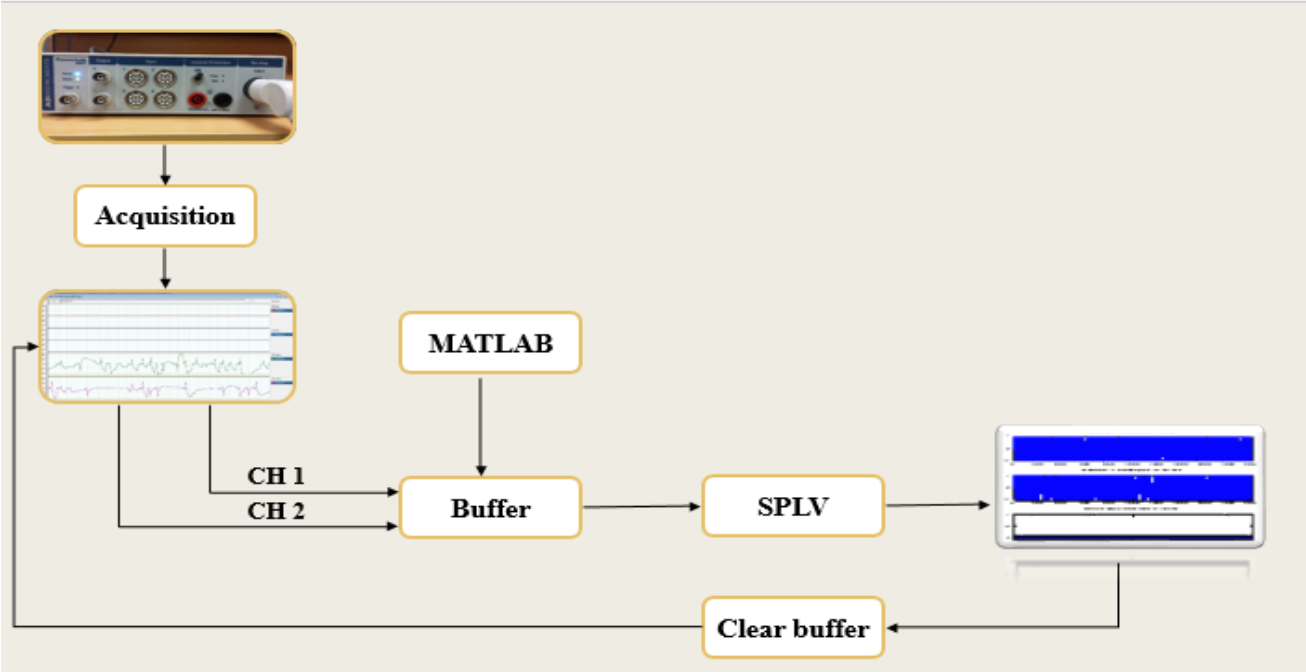

Figure 13: Real-time System Implementation block diagram

6.2 Signal Acquisition

Signals were acquired using dry surface electrodes filled with conductive gel. The hardware used for the conversion of analogue signals to digital signals was Powerlab® by ADInstruments. Powerlab is a powerful and user friendly system which is used to record and analyze data acquired from physiological signals. It allows recording from 4 channels

at a time. Powerlab hardware has a system time lag of 50-60 msec as mentioned in used manual for this hardware. After acquisition, analogue data is sent to a software called LabChart in which signal is amplified, filtered, sampled and then displayed as a digital signal on screen. The acquisition system is shown in detail in the block diagram below;

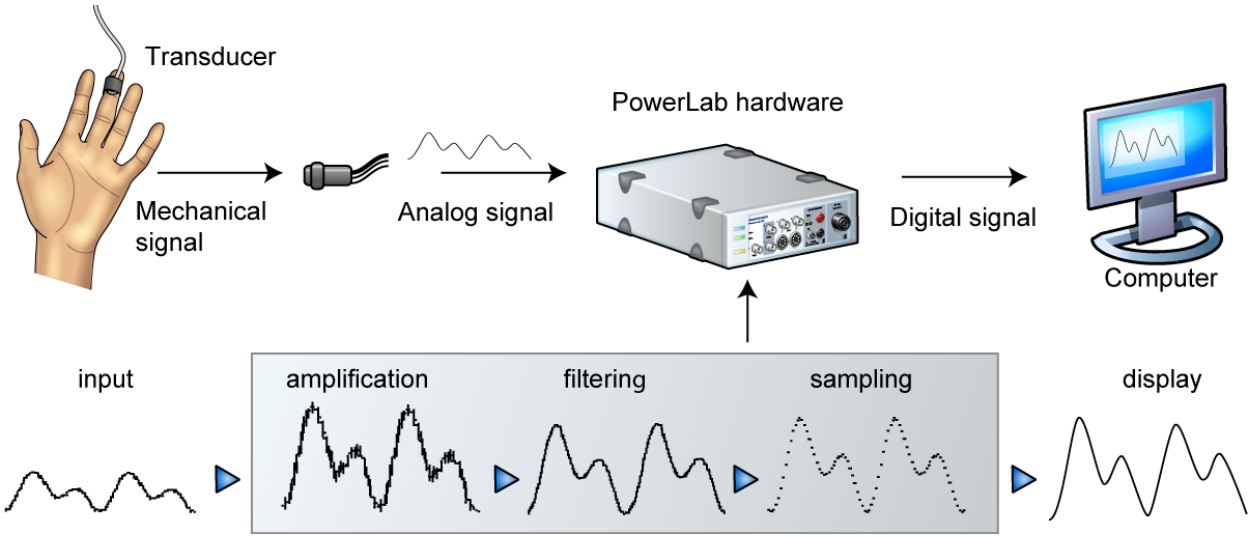

Figure 14: Signal Acquisition

6.3 Signal Processing

LabChart software is compatible with Matlab. Therefore, after receiving signal in LabChart, samples were sent to Matlab for the computation of SPLV. A buffer was created in Matlab that received data at a sampling rate of 1000 Hz from LabChart for 400 msec (400 samples). These samples were bandpass filtered; 8-13 Hz for EEG and 5-200 Hz for EMG signals; using a 50^{th} order FIR bandpass filter (a notch filter at 50 Hz was also used for EMG signals). These filtered signals were then used to compute analytical signals using Hilbert transform. The HT consists of a vector containing analytical amplitude as a real part, and analytical amplitude as imaginary part. Analytical phase were extracted for each

sample, which is actually the instantaneous phase for each signal. Relative phase was computed by subtracting the instantaneous phase of each signal within the buffer. These relative phase differences were averaged over total number of time points for the buffer i.e. 400 time points to get the SPLV value. A sample for the procedure of computing SPLV for a buffer of EMG signal is shown in the figure below.

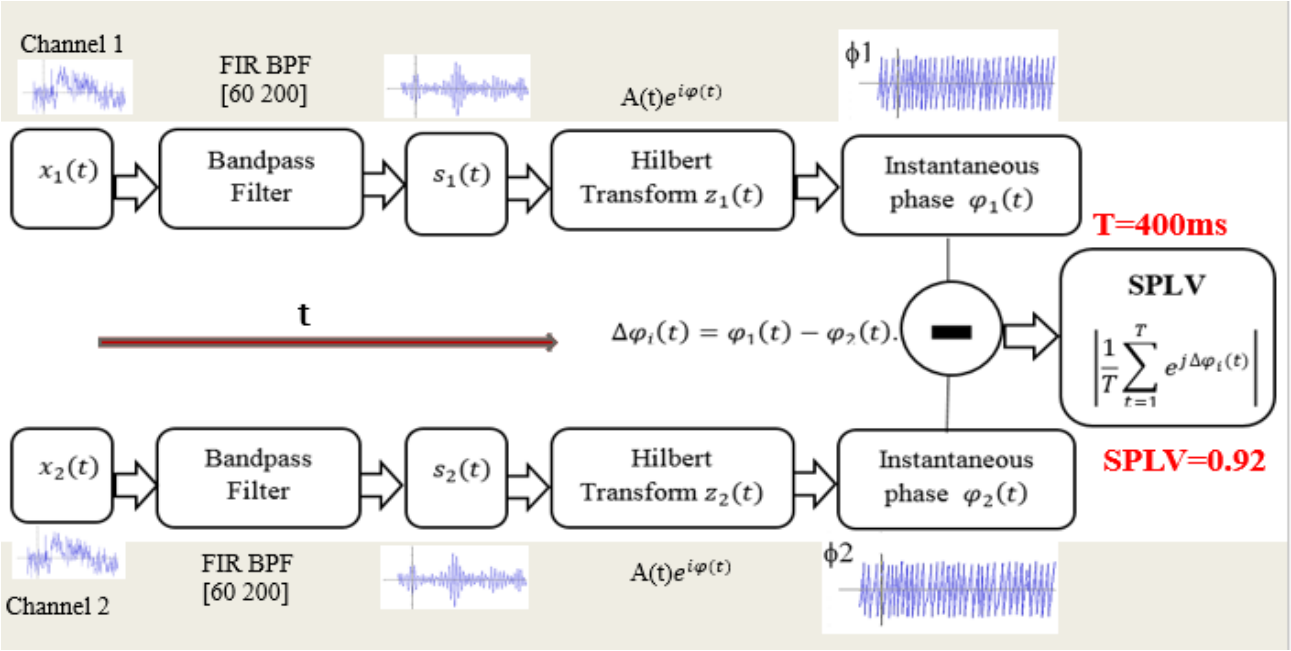

Figure 15: Real-time SPLV calculation for a buffer of 400 msec of EMG data

6.4 Experimental Setup

Real-time SPLV was implemented both for EEG and EMG signals. In both cases subject was asked to perform the same task i.e. finger tapping. Subjects were seated on a comfortable chair with their hands straight on an adjustable stool. Subjects heard a beep randomly after 750-850 msec. After hearing beep, the task was to tap index fingers of both hands either in-phase or out-of-phase. SPLV's were computed against each trigger (beep)

and displayed on the screen numerically and in the form of colored bars. These colored bars were assigned colors according to threshold values for SPLV's as shown below;

Table 5: SPLV Color Bars according to threshold values

SPLV Value	0-0.25	0.26-0.5	0.51-0.75	0.76-1.00
Color bar	RED	YELLOW	BLUE	GREEN

For EEG recordings, electrodes were placed at the left and right motor cortex to record motor rhythms when left and right hand fingers are tapped. Signals were band-pass filtered in mu-band (8-13) Hz in this case as motor activity is dominant in this frequency band. According to international 10-20 system, these motor points are named C3 and C4 respectively as shown in the Figure 16. For recording EMG signals, electrodes were placed at First Dorsal Interosseous (FDI) muscle and FDI mid belly points (Kleim, Kleim, & Cramer, 2007). In this case, signals were filtered in the frequency band of 5-200 Hz with a notch filter at 50 Hz. Although range of frequency for EMG signals range up to 500 Hz, it was found that dominant energies were present only in lower frequencies. An experimental setup for real-time EMG recordings is shown in Figure 17.

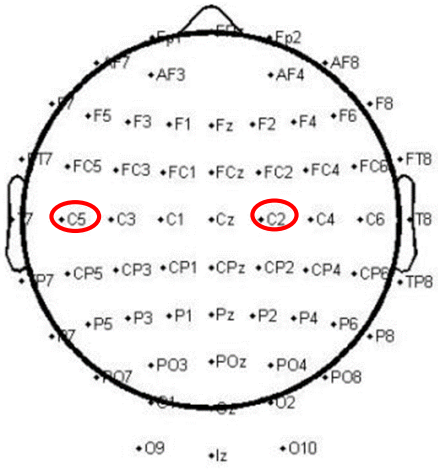

Figure 16: Electrodes placed at left and right motor cortex for EEG recordings

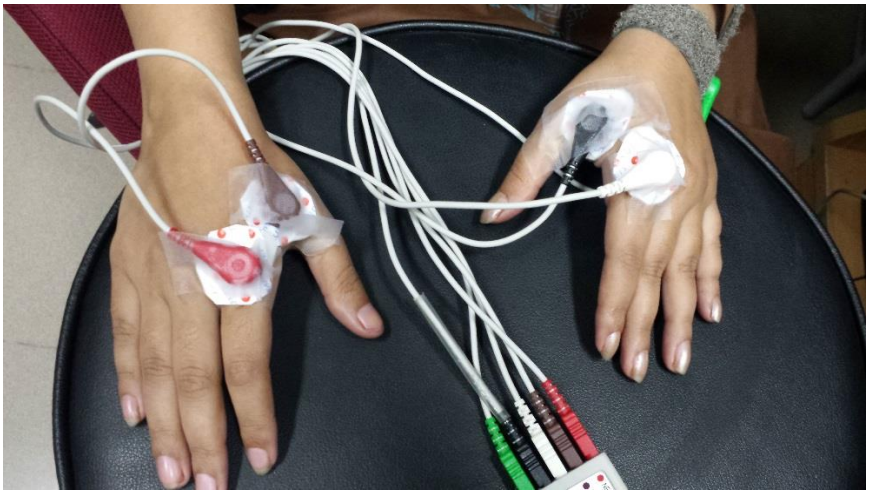

Figure 17: For EMG recordings, Electrodes are placed at first dorsal interosseous (FDI) muscle and FDI mid belly points (Kleim, Kleim, & Cramer, 2007)

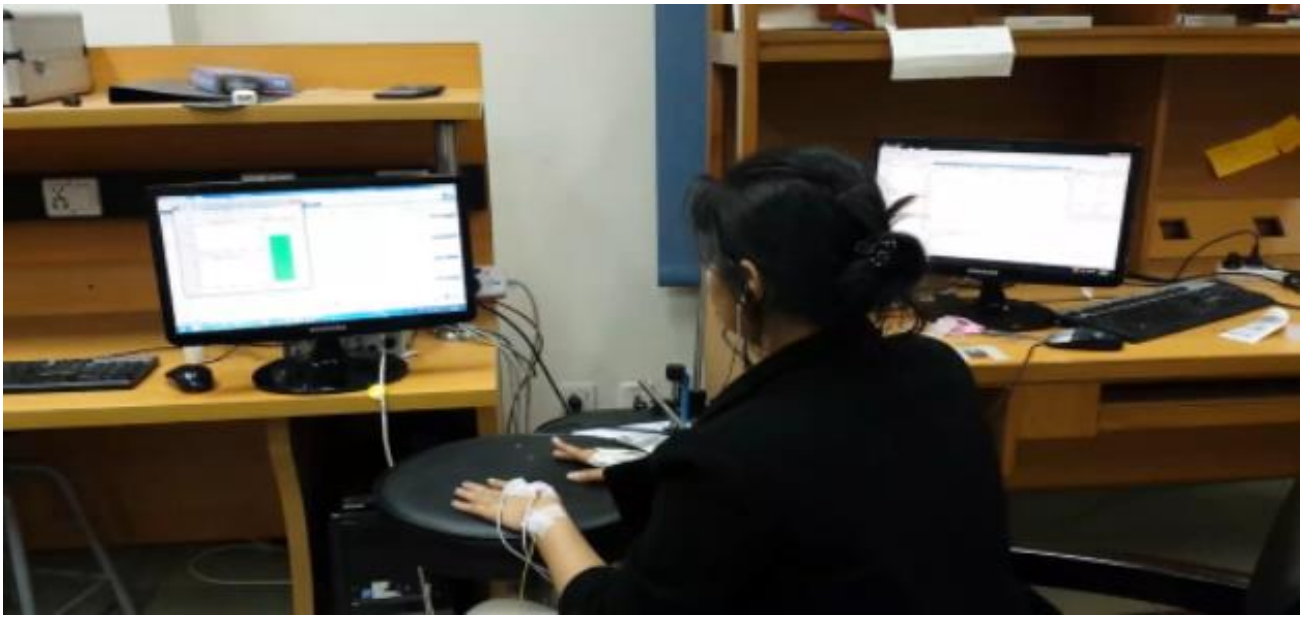

Figure 18: Experimental set-up for the real-time single trial phase synchrony detection of EMG signals.

PART 3

RESULTS

7. Results

7.1 Simulation

SPLV's were computed for every 200 msec interval of simulated signals. For sinusoid corresponding to channel 1, frequency was kept constant at 10 Hz throughout the time interval. For Sinusoid corresponding to channel 2, frequency was varied randomly between [8 13] Hz for every 200 msec interval. Table 6 shows the frequency value at every 200 msec interval for both channels and SPLV obtained for that interval. A graph showing SPLV at each 200 msec interval was plotted and is shown in the Figure 19 below;

Table 6: SPLV's for every 200 msec interval of simulated signals

Time interval (msec)	$\boldsymbol{x_1(t)}$ **(Hz)**	$\boldsymbol{x_2(t)}$ **(Hz)**	**SPLV**
0-200	10	11.8	0.19
201-400	10	8.5	0.16
401-600	10	12	0.05
601-800	10	10	1.00
801-1000	10	11	0.11
1001-1200	10	9	0.09
1201-1400	10	8.5	0.10
1401-1600	10	11	0.93
1601-1800	10	12.5	0.13

1801-2000	10	13	0.03

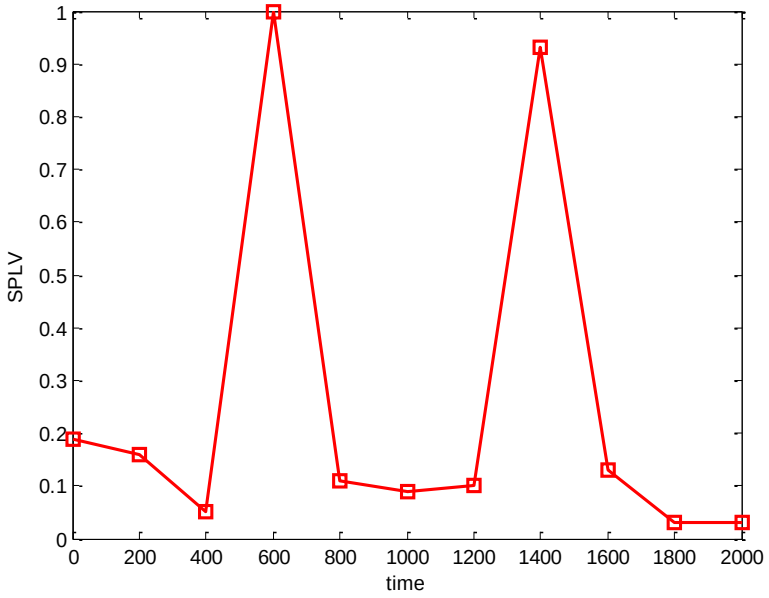

Figure 19: SPLV's for every 200 msec interval of simulated signals

Another graph was plotted for the simulated sinusoids such that Channel 1 frequency (F1) was kept constant to 10 Hz for 2000 msec time interval just like before. Channel 2 frequency (F2) was varied 50 times between [8-13] Hz for 2000 msec interval, each time with an increment of 0.1. The SPLV's obtained against channel pairs is shown in the Table 7 below and the graph for these values is plotted and shown in Figure 20.

Table 7: SPLV's with F2 varying between 8-13 Hz

F1 (Hz)	10	10	10	10	10	10	10	10	10	10
F2(Hz)	8.1	8.2	8.3	8.4	8.5	8.6	8.7	8.8	8.9	9.0
SPLV	0.0487	0.0769	0.0822	0.0592	0.0592	0.0664	0.1102	0.1196	0.0857	0.0857
F1(Hz)	10	10	10	10	10	10	10	10	10	10

F2(Hz)	9.1	9.2	9.3	9.4	9.5	9.6	9.7	9.8	9.9	10
SPLV	0.1037	0.1838	0.2100	0.1564	0.1564	0.2337	0.4999	0.7510	0.9359	1.000
F1(Hz)	10	10	10	10	10	10	10	10	10	10
F2(Hz)	10.1	10.2	10.3	10.4	10.5	10.6	10.7	10.8	10.9	11
SPLV	0.9355	0.7609	0.5099	0.2316	0.2316	0.1559	0.2198	0.1942	0.1037	0.1037
F1(Hz)	10	10	10	10	10	10	10	10	10	10
F2(Hz)	11.1	11.2	11.3	11.4	11.5	11.6	11.7	11.8	11.9	12
SPLV	0.0849	0.1293	0.1212	0.0667	0.0667	0.0583	0.0919	0.0886	0.0491	0.0491
F1(Hz)	10	10	10	10	10	10	10	10	10	10
F2(Hz)	12.1	12.2	12.3	12.4	12.5	12.6	12.7	12.8	12.9	13
SPLV	0.0443	0.0714	0.0701	0.0389	0.0389	0.0357	0.0584	0.0582	0.0323	0.0323

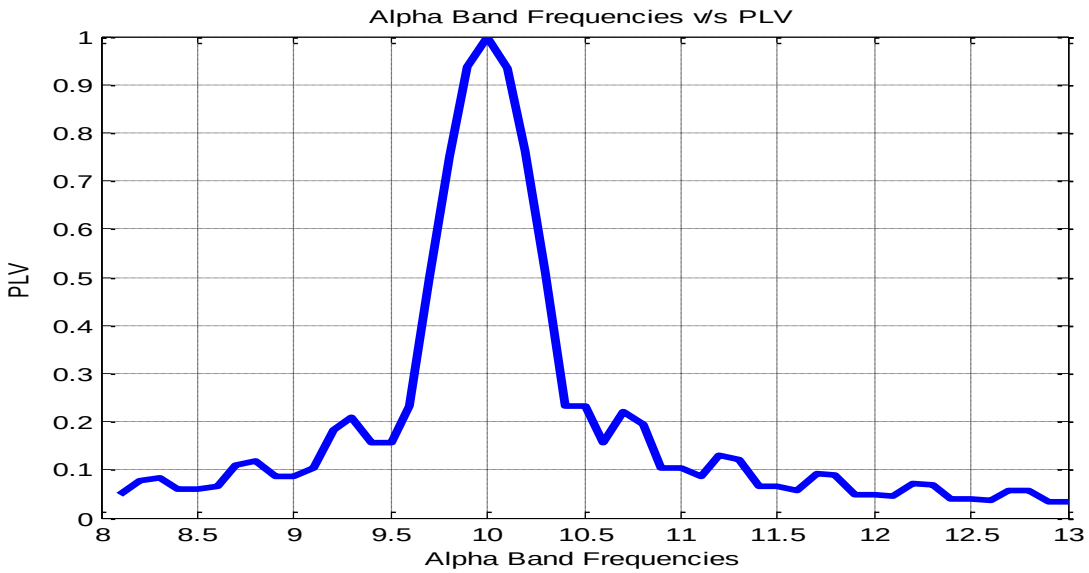

Figure 20: SPLV's with F2 varying between 8-13 Hz

7.2 Offline Phase

7.2.1 EEG Data

The total 512 trials of EEG data were divided into three learning phases; pre-learning, learning and post-learning phases. SPLV's were calculated for each trial and then averaged for total number of trials for respective phase. Out of 64 channels, 7 channel pairs were selected for SPLV calculation. Results for each learning phase 200 msec before and 200 msec after the presentation of trigger are shown in Table 8.

Table 8: SPLV: Pre-learning phase

Channel	Pre Trigger	Post Trigger
C3-C4	0.5075	0.5169
P3-P4	0.4829	0.5339
Fz-Pz	0.4311	0.4562
F3,F4	0.3823	0.3593
C3,CP3	0.7953	0.7812
C5,CP3	0.7322	0.7200
F5,PO4	0.2632	0.2513

Table 9: SPLV: Learning phase

Channel	Pre Trigger	Post Trigger
C3-C4	0.5075	0.5160
P3-P4	0.4829	0.5330
Fz,Pz	0.4311	0.4562

F3,F4	0.3823	0.3593
C3,CP3	0.7953	0.7812
C5,CP3	0.7322	0.7200
F5,PO4	0.2632	0.2513

Table 10: SPLV: Post-learning phase

Channel	**Pre Trigger**	**Post Trigger**
C3-C4	0.4707	0.5433
P3-P4	0.5046	0.5592
Fz,Pz	0.4166	0.4360
F3,F4	0.4491	0.4296
C3,CP3	0.7032	0.8184
C5,CP3	0.8003	0.7995
F5,PO4	0.2694	0.2753

A comparison was done between the three learning phases during pre-trigger and post-trigger phase for each channel pair selected. The results are shown graphically below;

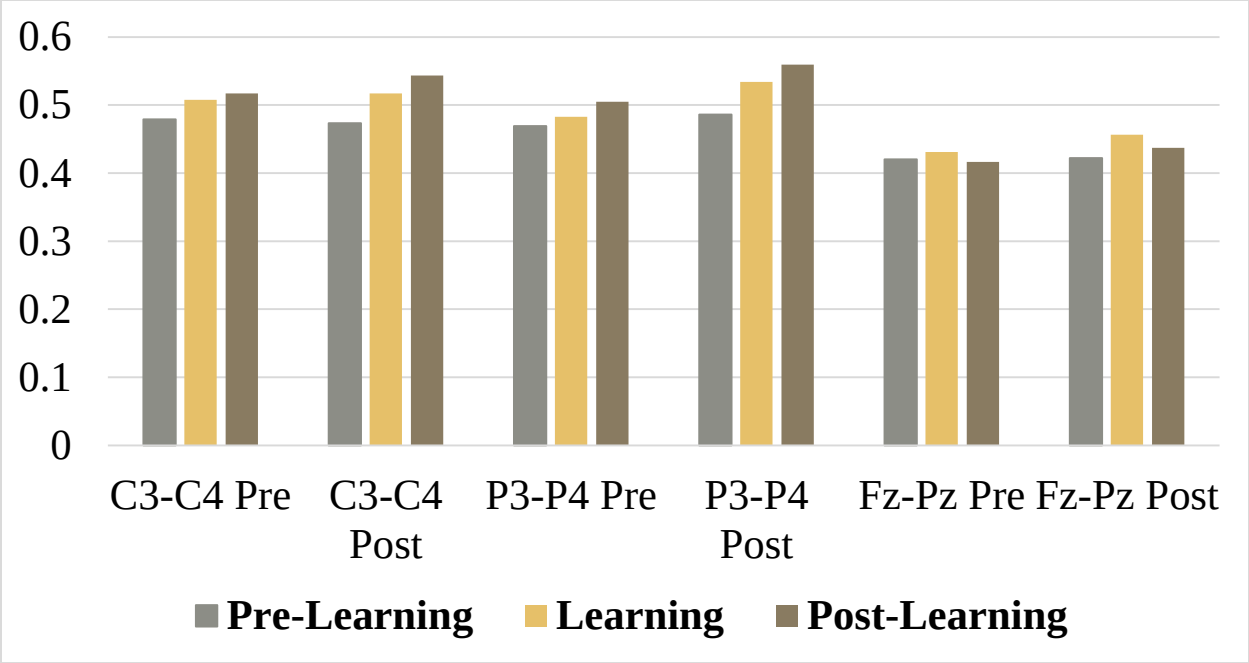

Figure 21: SPLV's Comparison during learning phases

7.3 Real-time Phase

Results were displayed in real-time continuously within 400 msec after trigger. Four windows were shown in display panel showing data received at channel 1 and 2, trigger point and a colored bar set according to threshold levels for SPLV. SPLV values were also displayed numerically over the colored bar. Since the results were shown in real-time, a few screen shots of the output window are shown here.

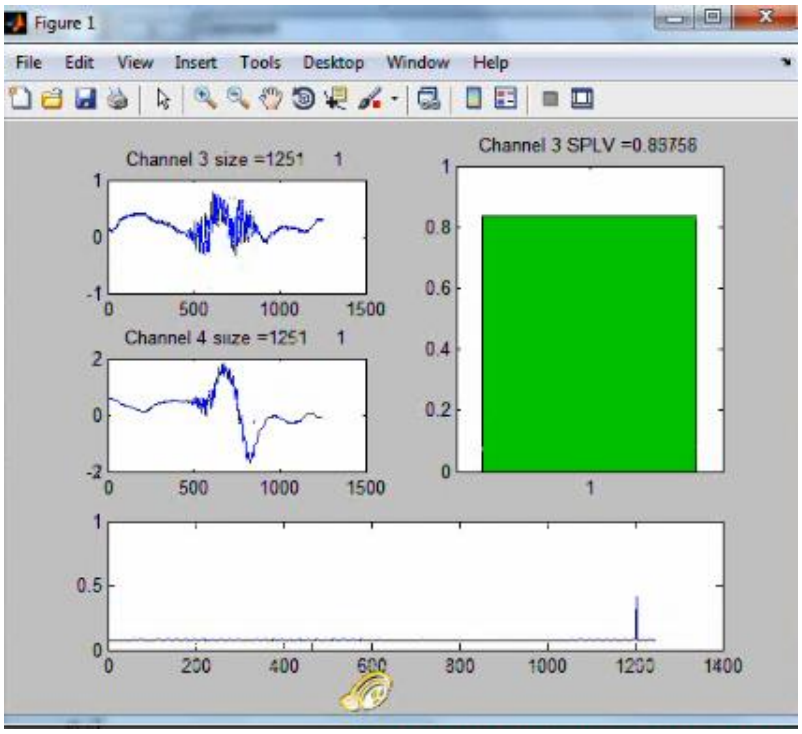

Figure 22: Real-time SPLV display (Sample # 1)

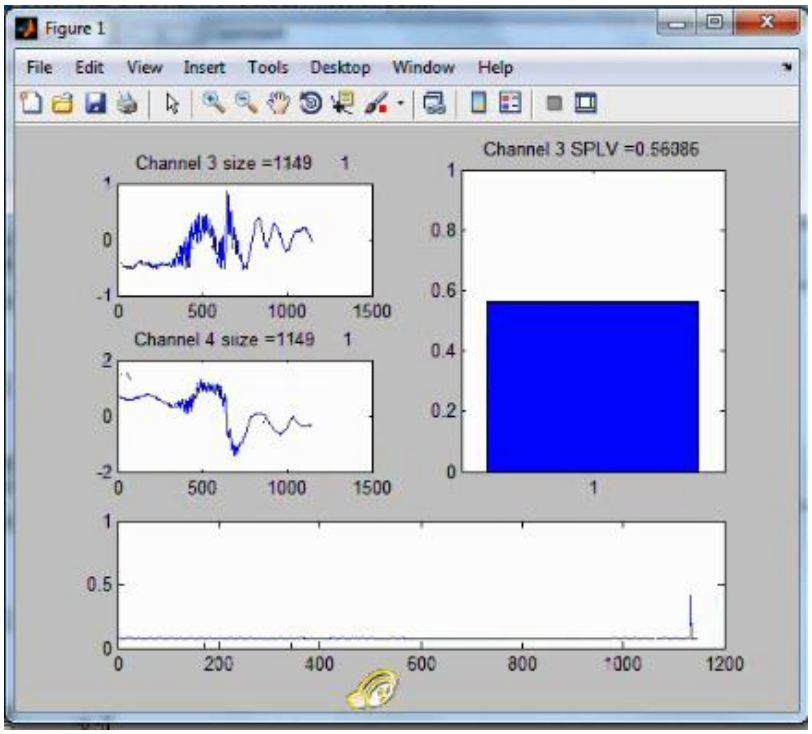

Figure 23: Real-time SPLV display (Sample # 2)

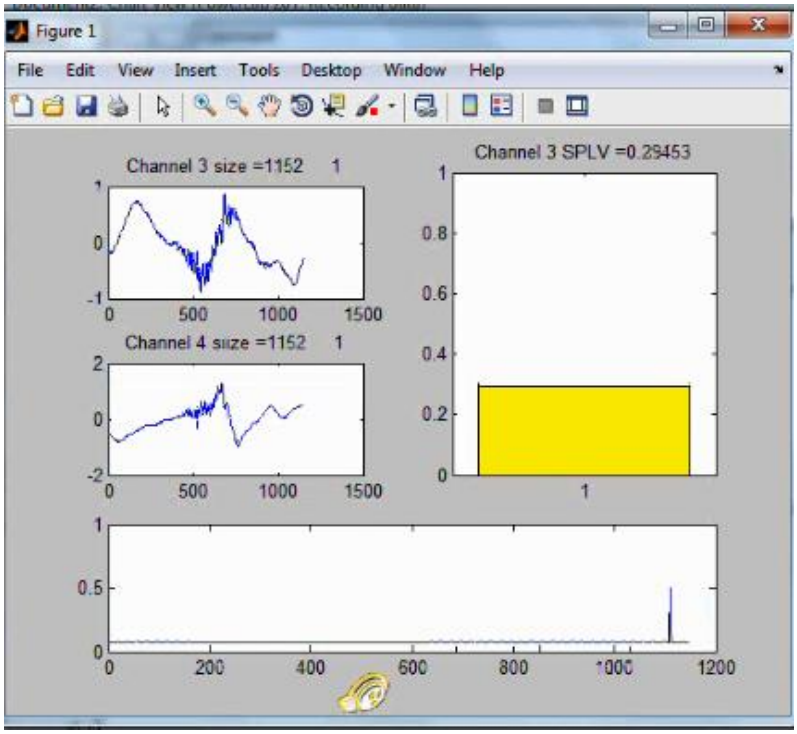

Figure 24: Real-time SPLV display (Sample # 3)

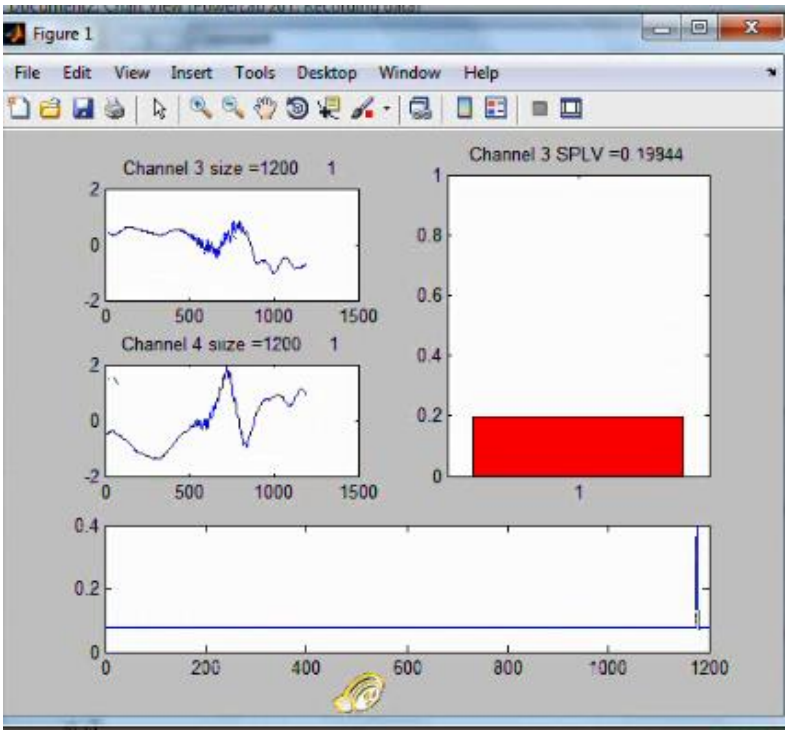

Figure 25: Real-time SPLV display (Sample # 4)

PART 4

DISCUSSION AND CONCLUSION

8. Discussion

8.1 Summary

The aim of this study is to compute level of synchronization for physiological signals by utilizing the phase of signals during single trials in real-time.

Physiological signals are recorded through electrodes; electrodes sense the electrical activity in biological systems. Synchronization among physiological signals is important for studying the communication mechanisms occurring within and between the physiological systems (e.g. EEG-EEG or EEG-EMG). The aim of this study is to compute the level of synchronization in physiological signals during single trials in real time.

Synchronization can be explained as the rhythmic adjustments of self-sustained oscillators as a result of coupling (e.g. classic clock pendulum). Phase synchronization is the relative temporal constancy of phases of two physiological signals that shows the electrical/oscillatory activity in the body. When this electrical/oscillatory activity gets time-locked to a stimulus event, it is called phase locking. A method called Single Trial Phase Locking Value (SPLV) has been used in this study for computation of synchrony levels among physiological signals during single trials in real-time.

Two types of physiological signals i.e. EEG and EMG are used in this study. First, SPLV method was developed for offline studies of phase synchronization for EEG data. (This data was recorded for another study). Based on SPLV results for offline data, SPLV offline method was optimized for use in real-time. For real-time, EEG and EMG signals were used following a finger tapping protocol. For EMG, SPLV's were computed by placing electrodes at mid-belly point and First Dorsal Interosseous (FDI) muscles of both

hands. For EEG, electrodes were placed at left and right sensory motor cortex (C3 and C4 according to international 10-20 system). Subjects were asked to perform same finger tapping task.

Real-time single trial phase synchronization can be used to study the plasticity induced in different parts of the brain. This study can be further utilized for neuro-muscular studies for rehabilitation applications. This method can also be used to study diverse functions such as motor activity, working memory, associative memory, attention, object recognition, awareness, perceptual organization or muscular activity during a specific task in real-time.

The overall system displayed results with a time lag of 130-170 msec in real time. The real-time display of phase synchronization level is helpful in understanding the level of interaction between physiological signals under study.

8.2 Why Phase Synchronization?

For any sinusoidal signal, two main factors are of interest, amplitude and phase. Every signal is actually a synodical signal in nature. That means it contains both factors of amplitude and phase. In case of physiological signals, phase corresponds to the firing rates which are actually the action potentials (Varela et al., 2001). A high firing rate for neurons shows greater number of action potentials. Phase synchronization is always computed in form of relative phase between two signals time-locked to a stimulus. Both signals are acquired from the two different regions of a physiological system. The extent to which the signals are phase synchronized, shows the extent of interaction between two regions.

8.3 Methodology

8.3.1 Why SPLV is used?

There are many techniques available in literature for the computation of phase synchronization. These methods are efficient and produces good results. However, these techniques are effective only for offline computation of phase synchronization. For the development of a real-time system, computational cost and temporal lag are the two major issues. Keeping this in mind, a major challenge was the development of such an algorithm that is not only computationally effective, but also efficient in terms of keeping the phase information intact.

Single-trial Phase Locking Value (SPLV) method was found to be best suitable method for real-time implementation. This method is already used on large scale for the computation of phase synchronization for offline data (Aydore et al., 2013; Lachaux et al., 2000). The major advantage of using this method is that it takes in to account only the instantaneous phase of the signals. No windowing is involved in this method. Instantaneous phase quantification allows us to compute SPLV for any desired length of trial. Also, because of the use of Hilbert Transform for obtaining analytical signal, the phase of the signal remains preserved, which is of course the major factor of system.

Phase Cross Coherence (PCC) is regarded as one of the best methods for computing phase synchronization for offline data. It utilizes the cross-spectral density of the frequency domain FFT signal. This method is not recommended for use in real-time system implementation because it involves an additional factor of amplitude, which is an extra computational cost and not affordable on real-time system.

8.3.2 Simulation

Simulation is always the first step before the actual implementation of the system. Two signals of 2000 msec length were stimulated having different frequencies. Frequency for the first signal was kept constant to 10 Hz, for a second signal frequency was varied after every 200 msec between 8-13 Hz randomly (Figure 6). A change in frequency shows a phase shift. Using this phase shift, the phase synchronization method was verified. It is evident that whenever the phase remains constant, the signals will remain synchronized. To verify this for SPLV method, a known frequency of 10 Hz was inserted at a known time interval (600-800 msec) of the second signals. This makes the frequency same for both signals during this interval, and so there is no phase shift. So, SPLV was found maximum during this interval (Table 6).

It was also found from Table 7 that SPLV tends to maximum value when the frequencies of both signals come close to each other and tends to minimum as soon as the frequency goes far apart. The trend of Figure 20 verifies this observation.

8.3.4 Offline Phase

The EEG data used for the offline system development, was divided into three learning phases. The task was performed in 512 trials. The task was performed 512 time will certain gaps. This suggests that learning to perform the given task should improve as the number of trials increase. SPLV's were computed for each trial and was then averaged over total number of trials for the particular learning phase (Table 8-10).

Six different types of electrode pairs were selected out of 64 channel data (Figure 12). Since this data was recorded for a visuomotor task, sensorimotor, frontal and parietal

cortex were involved during this task. To find out how these parts interact, SPLV's were calculated between left and right motor cortex, left and right parietal cortex, frontal and parietal cortex, left and right frontal cortex. Additionally, three other channel pairs were also checked to find out the cross talk between neighboring electrodes and its effect of SPLV. It was found that there is a high SPLV for signals from neighboring electrodes. This is because of the cross talk factor. For electrodes from two far away cortical regions that do not interact with each other, a very low SPLV was found.

SPLV comparison was done in pre-trigger and post-trigger phase. Pre-trigger analysis of signals corresponds to the movement preparation which actually starts few hundred milliseconds before the actual trigger. A graph was generated to know the trend of synchronization between three learning phase separately during pre-trigger and post-trigger for three channel pairs. It was found that as the number of trials increase, the synchronization among signals also increase. This shows a learning trend that subject has learnt the task and now the two brain regions are interacting more effectively (Figure 21).

8.3.5 Real-time Phase

The implementation of SPLV algorithm in real-time showed effective results. Utilizing the instantaneous phase of SPLV method, buffers were created for 400 msec and cleared after the display of SPLV on screen. During the in phase finger tapping task, both for EEG and EMG, SPLV's showed a maximum trend and remain above 0.5. As soon as the subject was asked to start tapping out of phase, the SPLV was dropped to less than 0.25.

8.3.5.1 Time Delay

A total time delay of 130-170 msec was found in the system. This includes both hardware and software delays. PowerLab® has an in-built system delay of 50-60 msec as mentioned in the manual for hardware. This time delay cannot be catered. Temporal lags on software side were minimized by keeping the algorithm as simple as possible. This time lag is acceptable for the system as the SPLV changes can easily be seen relative to task performance.

8.3.5.2 Filtering

Band pass filtering of physiological signals is a vital step and pre-processing stage for the computation of phase locking value. Filter selection was a challenging stage during the algorithm development. With an increase in filter order, a greater attenuation is produced in the beginning of signal, which can lead to loss of important information. An IIR filter with a lower order of 5-10 can be used to accomplish band pass filtering. However, IIR is an unstable filter and does not keep the phase information intact. It can be used for signal analysis of other types where phase information is not important, but in this study, phase is the most important factor. Therefore, a FIR filter was used in real-time system. FIR filter is a stable filter and keeps phase information preserved. The higher order issue was resolved by increasing the time points or samples. In this way, signal around trigger will remain preserved even after attenuation of starting signal.

8.4 Limitations and Implications

For the real-time system, buffer is cleared once new samples are available. Therefore, if one wants to study the trend of phase synchronization during the experiment,

an offline data analysis will be performed to obtain the complete graph. It is possible to develop an algorithm, that can draw a graph in real-time. This graph can also be used as a feedback for the subject to show him how better he is performing. Options are always available for the reduction of temporal lag. Minimizing this lag can improve the system performance.

9. Conclusion

This study presents a computationally efficient real-time phase synchronization detection system. This system can detect the level of synchronization between two physiological signals, and provides the extent to which the two regions of body interact. This system can be applied both in clinical and research domains. Being real-time system, provides an ease of analyzing physiological signals instantly.

References

Ahn, S., Zauber, S. E., Worth, R. M., Witt, T., & Rubchinsky, L. L. (2015). Interaction of synchronized dynamics in cortex and basal ganglia in Parkinson's disease. *European Journal of Neuroscience, 42*(5), 2164-2171.

Anwar, M. N., Navid, M. S., Khan, M., & Kitajo, K. (2015). A possible correlation between performance IQ, visuomotor adaptation ability and mu suppression. *Brain research, 1603*, 84-93.

Aydore, S., Pantazis, D., & Leahy, R. M. (2013). A note on the phase locking value and its properties. *Neuroimage, 74*, 231-244.

Boonstra, T. W., & Breakspear, M. (2012). Neural mechanisms of intermuscular coherence: implications for the rectification of surface electromyography. *Journal of neurophysiology, 107*(3), 796-807.

Bronzino, J. D. (1999). *Biomedical engineering handbook* (Vol. 2): CRC press.

Brunner, C., Scherer, R., Graimann, B., Supp, G., & Pfurtscheller, G. (2006). Online control of a brain-computer interface using phase synchronization. *Biomedical Engineering, IEEE Transactions on, 53*(12), 2501-2506.

Chang, Y.-J., Chou, C.-C., Chan, H.-L., Hsu, M.-J., Yeh, M.-Y., Fang, C.-Y., . . . Lien, H.-Y. (2012). Increases of quadriceps inter-muscular cross-correlation and coherence during exhausting stepping exercise. *Sensors, 12*(12), 16353-16367.

Chen, L. L., Madhavan, R., Rapoport, B. I., & Anderson, W. S. (2013). Real-time brain oscillation detection and phase-locked stimulation using autoregressive spectral estimation and time-series forward prediction. *Biomedical Engineering, IEEE Transactions on, 60*(3), 753-762.

Doesburg, S. M., & Ward, L. M. (2009). Synchronization between sources: Emerging methods for understanding large-scale functional networks in the human brain *Coordinated activity in the brain* (pp. 25-42): Springer.

Ewen, J. B., Lakshmanan, B. M., Hallett, M., Mostofsky, S. H., Crone, N. E., & Korzeniewska, A. (2015). Dynamics of functional and effective connectivity within human cortical motor control networks. *Clinical neurophysiology, 126*(5), 987-996.

Farmer, S. (1998). Rhythmicity, synchronization and binding in human and primate motor systems. *The Journal of Physiology, 509*(1), 3-14.

Glennon, M., Keane, M. A., Elliott, M. A., & Sauseng, P. (2015). Distributed cortical phase synchronization in the EEG reveals parallel attention and working memory processes involved in the attentional blink. *Cerebral Cortex*, bhv023.

Halliday, D. M., Conway, B. A., Farmer, S. F., & Rosenberg, J. R. (1998). Using electroencephalography to study functional coupling between cortical activity and electromyograms during voluntary contractions in humans. *Neuroscience letters, 241*(1), 5-8.

Herrera, A., Bernal, A., Isaza, D., & Adjouadi, M. (2004). *Design of an electrical prosthetic gripper using EMG and linear motion approach.* Paper presented at the Proceedings from the 17th Florida Conference on the Recent Advances in Robotics (FCRAR), Florida, USA.

Herwig, U., Satrapi, P., & Schönfeldt-Lecuona, C. (2003). Using the international 10-20 EEG system for positioning of transcranial magnetic stimulation. *Brain topography, 16*(2), 95-99.

Hsu, W.-Y. (2013). Single-trial motor imagery classification using asymmetry ratio, phase relation, wavelet-based fractal, and their selected combination. *International journal of neural systems, 23*(02), 1350007.

Hurtado, J. M., Rubchinsky, L. L., & Sigvardt, K. A. (2004). Statistical method for detection of phase-locking episodes in neural oscillations. *Journal of neurophysiology, 91*(4), 1883-1898.

Jovanov, E., Raskovic, D., Lords, A., Cox, P., Adhami, R., & Andrasik, F. (2003). *Synchronized physiological monitoring using a distributed wireless intelligent sensor system.* Paper presented at the Engineering in Medicine and Biology Society, 2003. Proceedings of the 25th Annual International Conference of the IEEE.

Keen, D. A., Chou, L.-W., Nordstrom, M. A., & Fuglevand, A. J. (2012). Short-term synchrony in diverse motor nuclei presumed to receive different extents of direct cortical input. *Journal of neurophysiology, 108*(12), 3264-3275.

Kim, K. H., Bang, S., & Kim, S. (2004). Emotion recognition system using short-term monitoring of physiological signals. *Medical and biological engineering and computing, 42*(3), 419-427.

Kleim, J. A., Kleim, E. D., & Cramer, S. C. (2007). Systematic assessment of training-induced changes in corticospinal output to hand using frameless stereotaxic transcranial magnetic stimulation. *Nature Protocols, 2*(7), 1675-1684.

Knyazeva, M. G., Carmeli, C., Khadivi, A., Ghika, J., Meuli, R., & Frackowiak, R. S. (2013). Evolution of source EEG synchronization in early Alzheimer's disease. *Neurobiology of aging, 34*(3), 694-705.

König, P., Engel, A. K., Roelfsema, P. R., & Singer, W. (1995). How precise is neuronal synchronization? *Neural Computation, 7*(3), 469-485.

Krusienski, D. J., McFarland, D. J., & Wolpaw, J. R. (2012). Value of amplitude, phase, and coherence features for a sensorimotor rhythm-based brain–computer interface. *Brain research bulletin, 87*(1), 130-134.

Lachaux, J.-P., Rodriguez, E., Le van Quyen, M., Lutz, A., Martinerie, J., & Varela, F. J. (2000). Studying single-trials of phase synchronous activity in the brain. *International Journal of Bifurcation and Chaos, 10*(10), 2429-2439.

Lachaux, J.-P., Rodriguez, E., Martinerie, J., & Varela, F. J. (1999). Measuring phase synchrony in brain signals. *Human brain mapping, 8*(4), 194-208.

Lamb, R., & Hobart, D. (1992). Anatomic and physiologic basis for surface electromyography. *Selected topics in surface electromyography for use in the occupational setting: Expert perspectives*, 6-21.

Liang, S., Choi, K.-S., Qin, J., Pang, W.-M., & Heng, P.-A. (2014). *Classification of motor imagery tasks using phase synchronization analysis of EEG based on multivariate empirical mode decomposition.* Paper presented at the Information Science and Technology (ICIST), 2014 4th IEEE International Conference on.

McAuley, J., & Marsden, C. (2000). Physiological and pathological tremors and rhythmic central motor control. *Brain, 123*(8), 1545-1567.

McKiernan, B. J., Marcario, J. K., Karrer, J. H., & Cheney, P. D. (2000). Correlations between corticomotoneuronal (CM) cell postspike effects and cell-target muscle covariation. *Journal of neurophysiology, 83*(1), 99-115.

Mormann, F., Lehnertz, K., David, P., & Elger, C. E. (2000). Mean phase coherence as a measure for phase synchronization and its application to the EEG of epilepsy patients. *Physica D: Nonlinear Phenomena, 144*(3), 358-369.

Nawab, S. H., Wotiz, R., Hochstein, L., & De Luca, C. (2002). *Next-generation decomposition of multi-channel EMG signals.* Paper presented at the Engineering in Medicine and Biology, 2002. 24th Annual Conference and the Annual Fall Meeting of the Biomedical Engineering Society EMBS/BMES Conference, 2002. Proceedings of the Second Joint.

Niedermeyer, E., & da Silva, F. L. (2005). *Electroencephalography: basic principles, clinical applications, and related fields*: Lippincott Williams & Wilkins.

Okamoto, M., Dan, H., Sakamoto, K., Takeo, K., Shimizu, K., Kohno, S., . . . Kohyama, K. (2004). Three-dimensional probabilistic anatomical cranio-cerebral correlation via the international 10–20 system oriented for transcranial functional brain mapping. *Neuroimage, 21*(1), 99-111.

Pfurtscheller, G., & Da Silva, F. L. (1999). Event-related EEG/MEG synchronization and desynchronization: basic principles. *Clinical neurophysiology, 110*(11), 1842-1857.

Quiroga, R. Q., Kraskov, A., Kreuz, T., & Grassberger, P. (2002). Performance of different synchronization measures in real data: a case study on electroencephalographic signals. *Physical Review E, 65*(4), 041903.

Rosenblum, M. G., Pikovsky, A. S., & Kurths, J. (1996). Phase synchronization of chaotic oscillators. *Physical review letters, 76*(11), 1804.

Sadeghi, S., MacKay, W. A., van Dam, R. M., & Thompson, M. (2011). Algorithm for real-time detection of signal patterns using phase synchrony: an application to an electrode array. *Measurement Science and Technology, 22*(2), 025802.

Scanziani, M., & Hausser, M. (2009). Electrophysiology in the age of light. *Nature, 461*(7266), 930-939.

Siriprayoonsak, S. (2005). Real-Time Measurement of Prehensile EMG Signals. *Unpublished master's thesis, San Diego State University, CA*.

Swann, N. C., de Hemptinne, C., Aron, A. R., Ostrem, J. L., Knight, R. T., & Starr, P. A. (2015). Elevated synchrony in Parkinson disease detected with electroencephalography. *Annals of neurology, 78*(5), 742-750.

Tass, P., Rosenblum, M., Weule, J., Kurths, J., Pikovsky, A., Volkmann, J., . . . Freund, H.-J. (1998). Detection of n: m phase locking from noisy data: application to magnetoencephalography. *Physical review letters, 81*(15), 3291.

Tatum, W. O. (2014). Ellen R. Grass Lecture: Extraordinary EEG. *The Neurodiagnostic Journal, 54*(1), 3-21.

Ushiyama, J., Katsu, M., Masakado, Y., Kimura, A., Liu, M., & Ushiba, J. (2011). Muscle fatigue-induced enhancement of corticomuscular coherence following sustained submaximal isometric contraction of the tibialis anterior muscle. *Journal of Applied Physiology, 110*(5), 1233-1240.

van Asseldonk, E. H., Campfens, S. F., Verwer, S. J., van Putten, M. J., & Stegeman, D. F. (2014). Reliability and agreement of intramuscular coherence in tibialis anterior muscle. *PloS one, 9*(2), e88428.

Varela, F., Lachaux, J.-P., Rodriguez, E., & Martinerie, J. (2001). The brainweb: phase synchronization and large-scale integration. *Nature reviews neuroscience, 2*(4), 229-239.

Vecchio, F., Miraglia, F., Curcio, G., Della Marca, G., Vollono, C., Mazzucchi, E., . . . Rossini, P. M. (2015). Cortical connectivity in fronto-temporal focal epilepsy from EEG analysis: A study via graph theory. *Clinical neurophysiology, 126*(6), 1108-1116.

Wang, L., Guo, X., Sun, J., Jin, Z., & Tong, S. (2012). *Cortical networks of hemianopia stroke patients: a graph theoretical analysis of EEG signals at resting state.* Paper presented at the Engineering in Medicine and Biology Society (EMBC), 2012 Annual International Conference of the IEEE.

Wang, L., Lu, A., Zhang, S., Niu, W., Zheng, F., & Gong, M. (2015). Fatigue-related electromyographic coherence and phase synchronization analysis between antagonistic elbow muscles. *Experimental brain research, 233*(3), 971-982.

Wang, Y., Hong, B., Gao, X., & Gao, S. (2006). *Phase synchrony measurement in motor cortex for classifying single-trial EEG during motor imagery.* Paper presented at the Engineering in Medicine and Biology Society, 2006. EMBS'06. 28th Annual International Conference of the IEEE.

Yeung, N., Bogacz, R., Holroyd, C. B., & Cohen, J. D. (2004). Detection of synchronized oscillations in the electroencephalogram: an evaluation of methods. *Psychophysiology, 41*(6), 822-832.